

# Intravital mesoscale optical imaging: challenges, techniques, and future perspectives

Mingrui Wang<sup>1,3</sup>, Jiamin Wu<sup>2,3</sup>, Qionghai Dai<sup>2,3</sup>✉

<sup>1</sup> Tsinghua Shenzhen International Graduate School, Tsinghua University, Shenzhen 518071, Guangdong, China

<sup>2</sup> Department of Automation, Tsinghua University, Beijing 100084, China

<sup>3</sup> Institute for Brain and Cognitive Sciences, Tsinghua University, Beijing 100084, China

Received: 17 February 2025 / Accepted: 23 April 2025

**Abstract** Intravital mesoscale imaging plays a crucial role in bridging the gap between cellular and organ-level investigations by enabling high-resolution visualization across large fields of view. Continuous advancements in optical microscopy have significantly improved imaging performance, yet fundamental challenges remain. Effective intravital mesoscale imaging requires a balance between spatial resolution, imaging speed, field of view, and while overcoming limitations such as scattering, aberrations, phototoxicity and photobleaching. This review summarizes key challenges in achieving high-performance intravital mesoscale optical imaging and provides an overview of advanced optical imaging techniques, including wide field, laser scanning, as well as computational imaging approaches. Despite these advancements, further improvements are necessary to address existing limitations and unlock new possibilities. Future developments will focus on enhancing imaging depth, further improving space bandwidth products, and integrating computational methods for real-time processing and large-scale data analysis, further advancing mesoscale imaging for biological research.

**Keywords** Intravital microscope, Mesoscale optical imaging, Space bandwidth product, Cellular dynamics, Tomography, Optical aberration

## INTRODUCTION

Visualizing cellular dynamics clearly at the mesoscale level is necessary for understanding various physiological processes. Many advanced optical microscopes for intravital imaging provide access to visualizing and understanding biological systems at high spatiotemporal resolution, facilitated by the development of optical design (Bennett 1943; Brady and Hagen 2009; McConnell *et al.* 2016; Negrean and Mansvelder 2014; Yan *et al.* 2017), mechanical engineering (Csencsics *et al.* 2020; Grandhe and Bandopadhyay, 2023), and computational processing (de Haan *et al.* 2020; Rivenson *et al.* 2017; Wang *et al.* 2019; Weigert *et al.* 2018). Various imaging strategies have been developed,

each with distinct advantages depending on the sample characteristics and imaging requirements. Wide-field imaging provides a rapid approach for planar imaging, enabling high temporal resolution even across large imaging fields of view (Werley *et al.* 2017). This technique is commonly used for thin samples and transparent specimens with fast dynamic processes. Laser scanning microscopes such as traditional two-photon microscopes (Denk *et al.* 1990), often provide clear imaging in scattering living samples due to their ability to physically reject out-of-focus signals. With the development of imaging techniques, microscopy has gradually advanced toward mesoscale and become more suitable for intravital imaging. Among the pioneering works in this field, Karel Svoboda and his colleague developed the two-photon mesoscope, enabling large-scale neural circuit imaging with

✉ Correspondence: qhdai@tsinghua.edu.cn (Q. Dai)

subcellular resolution (Sofroniew *et al.* 2016). Gail McConnell’s group introduced the Mesolens, which combines a large field of view with a high numerical aperture for volumetric imaging (McConnell *et al.* 2016). Our lab has also been a key leader in the invention of intravital mesoscale imaging with one of the pioneering works of the RUSH (real-time, ultra-large-scale, high-resolution) system which can be traced back to 2013, when we undertook a major scientific instrumentation project funded by the National Natural Science Foundation of China (Fan *et al.* 2019). All of these breakthroughs have laid the foundation for intravital mesoscope imaging, pushing the boundaries of mesoscale biological research. These systems often maintain high cellular spatial resolution while expanding the field of view (Fig. 1A) and achieving fast imaging speeds to capture dynamic cellular activities. Additionally, for complex intravital environments, it is crucial to address challenges such as scattering background and sample-induced aberrations

(Pittet and Weissleder 2011). Moreover, to enable long-term imaging, considerations must be given to laser-induced photobleaching of fluorescent proteins (Klonis *et al.* 2002) and photodamage to biological samples (Fig. 1B) (Hopt and Neher 2001; Magidson and Khodjakov 2013). Therefore, mesoscale intravital imaging requires systemic improvement of all aspects of traditional optical microscopy, including the field of view, resolution, 3D imaging speed, low phototoxicity, aberration robustness, and high fidelity against background fluorescence, leading to grand challenges in the optics field.

This review will introduce intravital mesoscope imaging methods. First, the challenges associated with achieving high-performance intravital mesoscale imaging will be discussed. Then, advanced mesoscale imaging techniques will be presented, highlighting their principles, key characteristics, and suitable applications. Finally, the review will explore the future potentials of intravital mesoscope, discussing the

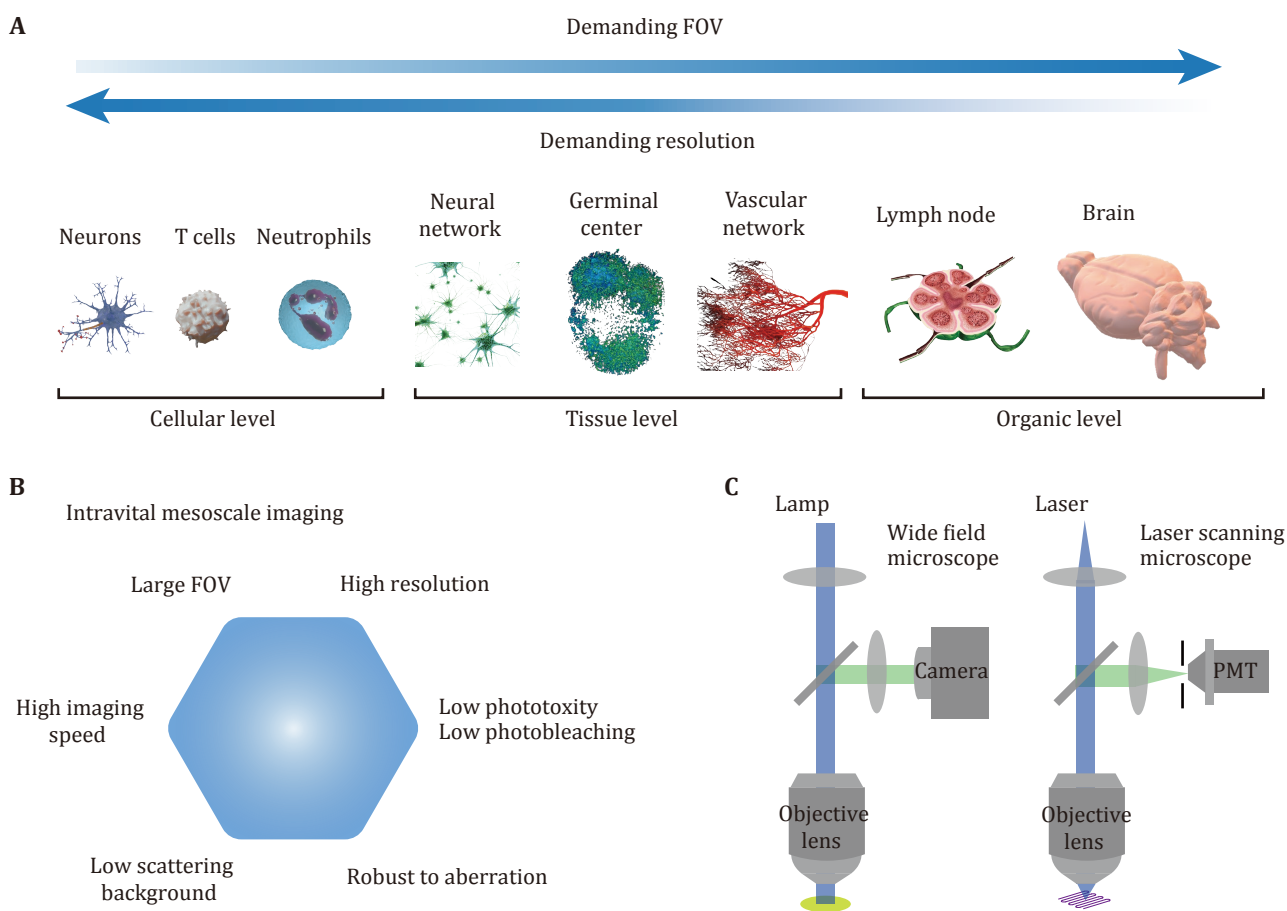


**Fig. 1** **A** Illustration of biological frameworks which inherently operate across multiple scales, ranging from the cellular to the organ level. **B** Basic requirements of intravital mesoscope imaging. **C** Comparison of the framework between wide field imaging and laser scanning imaging

remaining limitations and key challenges that need to be addressed for further enhancement, analysis and applications.

### CHALLENGES OF INTRAVITAL MESOSCALE IMAGING

To capture the entire landscape of biological systems, microscopes need to be equipped with a large field of view (FOV), typically ranging from several millimeters to even centimeter scale, while maintaining high

resolution to achieve cellular-level details. The amount of information provided by optical imaging techniques is quantified as the space bandwidth product (SBP) (Lohmann *et al.* 1996; Mendlovic *et al.* 1997), with a higher SBP indicating greater information acquisition. However, two key factors limit the increase of SBP: first, the sampling rate of the imaging system (Orth and Crozier 2013); second, the performance of optical access (Fig. 2A), as the resolution is constrained by optical diffraction, and system aberrations tend to be larger as the FOV expands (Lohmann 1989).

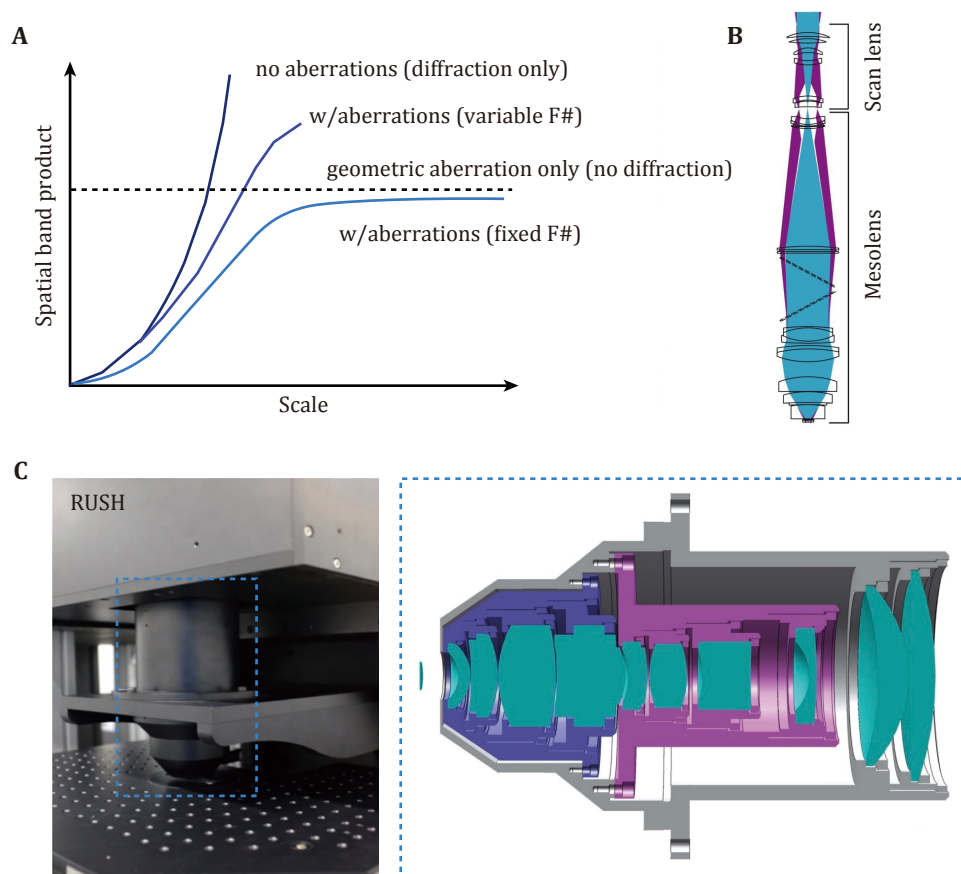


**Fig. 2** **A** Space-bandwidth product of an optical system as a function of scale for no aberrations (top), with aberration (variable F#), no diffraction (dashed line) and with aberration (fixed F#) (bottom) (Lohmann 1989). **B** Optical design of mesolens objective lens (McConnell *et al.* 2016). **C** Optical design of objective lens of RUSH system. Left, photograph of the objective lens. Right, optical design details (Fan *et al.* 2019)

To effectively record cellular dynamics in living samples – such as neutrophil migration within blood vessels (Lerman and Kim 2015; Salvermoser *et al.* 2018; Xu *et al.* 2022), calcium signaling (Augustine *et al.* 2003; Berridge 1998) or voltage fluctuations representing neuronal activity (Peterka *et al.* 2011) – imaging

systems must achieve high-speed acquisition, typically ranging from one to hundreds of frames per second (fps). This combination of a large FOV, high resolution, and fast imaging speed is critical for capturing the complex and dynamic processes occurring in biological systems.

Most living samples are composed of highly scattering tissues, creating complex imaging conditions that hinder the detection of signals, especially from deeper layers (Cheng *et al.* 2020). The scattering not only limits imaging depth but also generates substantial background noise, in contrast to the clear environment of transparent *ex vivo* samples, thereby significantly reducing the signal-to-background ratio (SBR) (Zhang *et al.* 2021a). Laser scanning microscopy addresses this challenge by utilizing point-scanning techniques and effectively rejecting out-of-focus light, enabling the acquisition of clear cellular images even in scattering environments (Davidovits and Egger 1971; Denk *et al.* 1990; Minsky 1988; Otsu *et al.* 2008). Besides, biological samples often introduce considerable optical aberrations due to refractive index mismatches. These aberrations further degrade image quality, posing additional challenges for high-resolution intravital imaging (Schwertner *et al.* 2004).

A wide range of biological processes, such as tumor metastasis (Condeelis and Weissleder 2010; Khanna and Hunter 2005), germinal center formation in lymph nodes (Gonzalez-Figueroa *et al.* 2021; MacLennan 1994; Victora *et al.* 2010) and other immune response after organ injury (An *et al.* 2025) require extended periods to complete, ranging from several hours to even days, often accompanied by complex and dynamic changes. However, prolonged exposure to light introduces phototoxicity effects (Gottschalk *et al.* 2015), leading to cellular damage or even cell death. Photobleaching is another critical concern. Fluorescent proteins or dyes, commonly used to enhance imaging contrast (Prasher 1995; Shimomura *et al.* 1962), gradually lose their fluorescence under continuous illumination, thereby limiting the duration and quality of imaging sessions. Currently, the intravital mesoscope must carefully balance these factors. Therefore, optimizing imaging systems to minimize light-induced damage while maintaining sufficient image quality is a key challenge in long-term intravital imaging.

Nowadays, with the advancement of imaging technologies, various mesoscale imaging methods have been developed to address the aforementioned challenges, making them more suitable for intravital applications. To better illustrate the capabilities of different mesoscale imaging techniques, Table 1 summarizes key performance metrics, including spatial resolution, temporal resolution, and FOV. This comparison provides insights into the strengths of each imaging system to help identify the most suitable technique for specific intravital applications. This review will delve into the details of these mesoscale imaging techniques, discussing their technological

developments, optimal application scenarios, distinctive characteristics, and the key methodologies that underpin their performance.

## TECHNIQUES OF INTRAVITAL MESOSCALE IMAGING

Current imaging techniques for intravital mesoscale imaging can be broadly categorized into two approaches: wide field imaging and laser scanning imaging (Fig. 1C) (Schneckenburger and Richter 2021). Besides, advancements in computational imaging have further enhanced both imaging approaches (Dong *et al.* 2023; Mait *et al.* 2018; Zhao *et al.* 2023), offering solutions to overcome inherent trade-offs between resolution, speed, and imaging depth.

Wide field imaging involves uniformly illuminating the entire observation area at once, followed by capturing the image using a fast photon array detector, such as a high-speed CMOS, CCD or sCMOS camera. This approach allows for rapid acquisition of large-area images, making it highly efficient for visualizing extensive regions of tissues or organs (Werley *et al.* 2017; Zheng *et al.* 2024). However, wide field imaging is often hindered by out-of-focus background signals or scattering from within the sample, which can reduce image contrast and obscure fine details.

In contrast, laser scanning methods, such as confocal microscopy (Davidovits and Egger 1971; Sheppard and Choudhury 1977) or nonlinear techniques like two-photon excitation microscopy (Denk *et al.* 1990; Helmchen and Denk 2005), operate by sequentially exciting and detecting signals from individual points within the biological sample. This point-by-point scanning approach effectively suppresses background fluorescence and scattered light, yielding higher contrast images with improved optical sectioning. Nevertheless, the speed of laser scanning methods is inherently limited due to the point-by-point data acquisition. This limitation becomes particularly pronounced when imaging larger fields of view, as the increased number of sampling points significantly extends the acquisition time.

The trade-offs between wide field and laser scanning methods highlight the challenges of achieving both high-speed and high-contrast imaging intravitaly, especially when imaging at the mesoscale level. Based on their imaging principles and characteristics, these techniques are suited to different application scenarios (Oleksiievets *et al.* 2022; Swedlow *et al.* 2002). With ongoing advancements in imaging technology, both approaches are continuously evolving to enhance their strengths while addressing their inherent limitations.

**Table 1** Comparison of representative intravital mesoscale imaging techniques in terms of their spatial resolution, temporal resolution, and FOV across different modalities

Year	Name of techniques	Reference	Basic parameters				Simple description
			FOV (mm)	Resolution ( $\mu\text{m}$ )	Imaging speed (fps)	Effective pixel (voxel) acquisition rate (kHz)	
2016	2p-RAM	Sofroniew <i>et al.</i> 2016	$\Phi 5 \times 1$	Lateral: 0.66; Axial: 4.09	0.7	$7.7 \times 10^3$	Two photon imaging with subcellular resolution
2016	Confocal Mesolens	McConnell <i>et al.</i> 2016	$\Phi 6 \times 3$	Lateral: 0.8; Axial: 8	0.005	$3.3 \times 10^2$	Confocal imaging
2016	Treapn2p	Stirman <i>et al.</i> 2016	$\Phi 3.5$	Lateral: 1.2; Axial: 12	0.1	$6.7 \times 10^2$	Two photon imaging with temporal multiplexing
2017	Firefly	Werley <i>et al.</i> 2017	$\Phi 6$	Lateral: 7	100	$3.4 \times 10^4$	Wide field imaging
2019	RUSH	Fan <i>et al.</i> 2019	$12 \times 10$	Lateral: 0.8	30	$5.6 \times 10^6$	Wide field imaging, 35 sCMOS for detection
2021	FASHIO-2PM	Ota <i>et al.</i> 2021	$3 \times 3$	Lateral: 1.61; Axial: 7.07	7.5	$5.9 \times 10^3$	Two photon imaging
2021	Quadroscope	Clough <i>et al.</i> 2021	$\Phi 4.8$	Lateral: 0.91; Axial: 10.5	30	$5.1 \times 10^3$	Two photon imaging with temporal multiplexing
2021	Diesel2p	Yu <i>et al.</i> 2021	$\Phi 5$	Lateral: 1; Axial: 8	3.85	$1.7 \times 10^4$	Two photon imaging with temporal multiplexing and AO
2021	LBM	Demas <i>et al.</i> 2021	$5.4 \times 6 \times 0.5$	Lateral: $\sim 5$	2	$3.9 \times 10^4$	Two photon imaging with axially separated and temporally distinct foci
2022	MINI2P	Zong <i>et al.</i> 2022	$5 \times 5 \times 0.16$	Lateral: $\sim 1.2$ ; Axial: $\sim 14$	15 (single FOV)	$2.9 \times 10^4$	Miniature head-mounted 2p mesoscope
2023	3D-RAPID	Zhou <i>et al.</i> 2023	$12 \times 10.8 \times 0.9$	Lateral: 25	15	$2.8 \times 10^4$	Wide field imaging, 54 sCMOS for detection
2023	Mesosopic OPM	Daetwyler <i>et al.</i> 2023	$3.7 \times 1.5 \times 1$	Lateral: 2.3; Axial: 9.2	5	$5.7 \times 10^5$	Single objective lens light sheet imaging
2024	RA-WiFi	Shi <i>et al.</i> 2024	$12.8 \times 12.8$	Lateral: 2.18	2	$6.8 \times 10^4$	Random access wide field imaging with AO correction
2024	SOMM	Zhang <i>et al.</i> 2024b	$3.6 \times 3.6 \times 0.3$	Lateral: 4	16	$1.3 \times 10^4$	Miniature mesoscope
2024	RUSH3D	Zhang <i>et al.</i> 2024a	$8 \times 6 \times 0.4$	Lateral: 2.6; Axial: 6	20	$7.4 \times 10^7$	Scanning light field imaging, DAO for aberration correction

For instance, innovations in wide field imaging aim to mitigate background and scattering effects through techniques like structured illumination (Gustafsson 2000; Gustafsson *et al.* 2008) or light-sheet illumination (Huisken *et al.* 2004). Similarly, laser scanning methods are being improved with faster scanning mechanisms, such as resonant scanning or multi-point excitation with parallelized beam paths (Nikolenko *et al.* 2008;

Otomo *et al.* 2015; Yang and Yuste 2018) or temporal focusing (Vaziri and Shank 2010), to overcome speed limitations. These developments enable both wide field and laser scanning techniques to better meet the demands of intravital mesoscale imaging, making them increasingly versatile for current applications.

Beyond advancements in optical system, computational imaging has emerged as a powerful approach to

enhance both wide field and laser scanning techniques. Techniques such as light-field microscopy (Prevedel *et al.* 2014), scanning light field microscopy (Lu *et al.* 2025; Wu *et al.* 2021; Zhang *et al.* 2024a), compressive sensing-based reconstruction (Wen *et al.* 2019), and deep-learning-assisted tomography (Wang *et al.* 2021) have demonstrated remarkable potential in overcoming trade-offs between resolution, speed and FOV. Computational imaging approaches can also compensate for scattering effects and aberrations (Zhang *et al.* 2024a), making them particularly valuable for intravital mesoscale imaging applications.

### Wide field imaging

Wide field imaging usually illuminates and captures the entire field of view simultaneously. Wide field framework is easy to set up and widely applicable across various scenarios (Holtmaat *et al.* 2009; Xiao *et al.* 2024; Yang *et al.* 2010; Zheng *et al.* 2013, 2024). It is not only utilized in table-set microscopes for mesoscale imaging but also adapted for miniaturized devices, such as head-mounted microscopes (de Groot *et al.* 2020; Guo *et al.* 2023; Rynes *et al.* 2021; Zhang *et al.* 2024b), enabling large FOV imaging in freely behaving animals.

For mesoscale microscope imaging, we often need higher SBP to cover more information (Park *et al.* 2021). In practice, two key factors limit the SBP, the sampling rate of the imaging sensor and system optical diffraction aberration. Nowadays, advanced high-resolution CMOS sensors can accommodate a large number of pixels, and the use of camera arrays (Fan *et al.* 2019; Zhou *et al.* 2023) further enhances spatial digital sampling rates. More commercial and customized objective lenses (Kim *et al.* 2016; McConnell *et al.* 2016) are being developed to expand the FOV and minimize optical aberrations, such as astigmatism and field curvature, particularly at the edges of the imaging field (Welford 2017). McConnell *et al.* developed a complex mesoscale lens (Fig. 2B) that comprised 15 optical elements for aberration corrections (McConnell *et al.* 2016). Fan *et al.* developed the RUSH system, which features a centimeter-scale field of view and a spatial resolution of 0.8 micrometers (Fan *et al.* 2019). The system employs a custom-designed large lens that effectively corrects aberrations across a wide field (Fig. 2C). Additionally, it integrates a camera array with 35 cameras for simultaneous imaging, significantly enhancing spatial sampling. Notably, it is the world's first real-time gigapixel fluorescence microscope for intravital imaging and remains among the leading systems in data throughput. A three-dimensional (3D) parallelized computational wide field mesoscope

implements 54 cameras for large scale and not only increases the spatial sampling rate (Zhou *et al.* 2023), but also captures information from different views for 3D reconstruction. These advancements have significantly improved the imaging system's SBP, enabling rapid acquisition of detailed information across a large FOV.

However, a large FOV also introduces complex challenges, such as defocus aberrations caused by curved surfaces, blank regions that record unnecessary data, and more complex higher-order aberrations induced by mismatched refractive indices (Potsaid *et al.* 2005). Several systems implement digital micromirror devices (DMD) for structure illumination, a series of different thicknesses of glass (Xie *et al.* 2024) or electrically tunable lens (ETL) (Shi *et al.* 2024) and deformable mirrors for refocusing specific regions. For example, Shi *et al.* developed RA-WiFi (random-access wide field) mesoscope using a commercial objective lens, extending the working distance to achieve a larger FOV enabling imaging on a scale of one square centimeter and implementing a scanning mirror to record a specific region, which is illuminated by the reflection of DMD, and use ETL and deformable mirror for the aberration correction mainly for defocus (Shi *et al.* 2024). These methods have made imaging systems more flexible, enhancing the proportion of useful information and making them better suited for more complex intravital imaging environments.

Epi-illumination in wide field microscopy is convenient for system setup and sample placement during experiments, but the out-of-focus background can significantly reduce the SBR. Light-sheet microscopy typically illuminates the focal plane from a direction orthogonal to the imaging objective, effectively reducing the fluorescence background (Huisken *et al.* 2004). By scanning either the objective lens or the sample stage, it enables the reconstruction of a 3D image of the specimen. However, the mechanical scanning of the objective lens and sample stage limits imaging speed, making this approach more commonly used for imaging cleared tissues. Advanced imaging systems now incorporate multi-plane excitation (Ren *et al.* 2020), extended depth of field (DOF) (Tomer *et al.* 2015), and galvo-mirror-scanned light sheets to increase 3D imaging speed for intravital applications, enabling the capture of cellular dynamics, such as recording neuronal activity across an entire zebrafish at 5 Hz (Tomer *et al.* 2015). To eliminate the lateral constraints imposed by the illumination objective lens, Dunsby introduced an approach where an oblique light sheet is emitted from the edge of the imaging objective, enabling single-objective light-sheet microscopy

(Dunsby 2008). These systems typically require two objective lenses for 1:1 imaging with minimal aberration, allowing the secondary objective to capture the illuminated plane from a perpendicular angle. To image a living sample at video rate, the light-sheet scanning galvo-mirror is positioned at the back focal plane, ensuring that the image plane remains stationary during acquisition (Bouchard *et al.* 2015; Kumar *et al.* 2018; Kumar and Kozorovitskiy 2019; Voleti *et al.* 2019). To achieve mesoscale imaging with a low-NA objective lens, several methods incorporate diffraction gratings (Hoffmann and Judkewitz 2019), blaze gratings

(Hoffmann *et al.* 2023; Shao *et al.* 2022), or high-refractive-index media (Daetwyler *et al.* 2023) to enhance light collection efficiency in single-objective light-sheet microscopy (Figs. 3A and 3B). These methods enable higher SBR 3D mesoscale imaging at video rate for commonly used model organisms. For example, they have been applied to imaging transparent samples, capturing neuronal activity in *C. elegans* (Voleti *et al.* 2019) and zebrafish (Daetwyler *et al.* 2023), and even visualizing cellular dynamic processes in the scattering tissue of the mouse cortex (Bouchard *et al.* 2015; Wang *et al.* 2023).

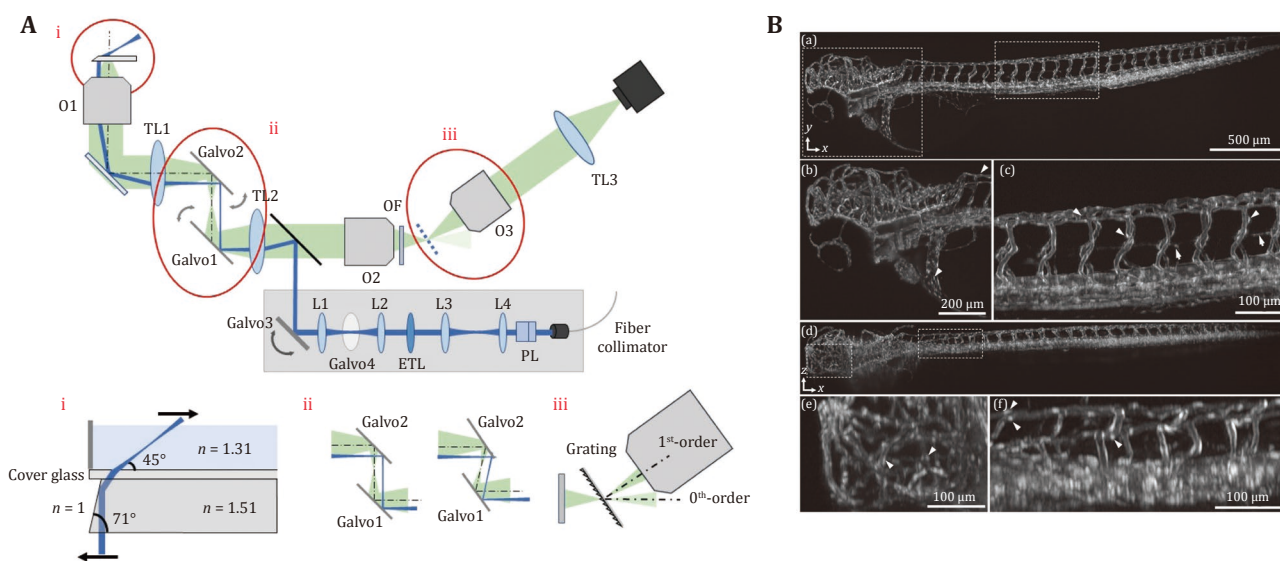


**Fig. 3** **A** Schematic setup of the mesoscopic oblique plane microscope. O1–O3, primary, secondary, and tertiary objectives; TL1–TL3, primary, secondary, and tertiary tube lenses; OF, optical flat. Inset (i) shows detail of the microprism that reflects the light sheet into the sample. Inset (ii) shows the working principle of the image space scanning. Inset (iii) shows how the blazed diffraction grating diffracts the first order towards the primary objective. **B** Imaging of zebrafish vasculature. Fluorescently labeled vasculature, in a three days post fertilization (dpf) zebrafish larva, as imaged with our mesoscopic OPM. (a)  $x$ - $y$  maximum intensity projection of the entire zebrafish with (b, c) magnified views (head and tail vasculature) of the boxed regions in (a). Arrowheads indicate selected endothelial nuclei, and arrows point to parachordal lymphangioblasts. (d)  $x$ - $z$  maximum intensity with (e, f)  $x$ - $z$  maximum intensity projected magnified views (head and tail vasculature) of the boxed regions in (d). Arrowheads indicate selected endothelial nuclei (Daetwyler *et al.* 2023)

Overall, wide field imaging techniques, including advanced light-sheet microscopy, have significantly improved the SBP, speed and SBR for mesoscale intravital imaging. These methods enable high-speed, large-scale imaging across various biological models typically with simple optical setups, from transparent organisms to scattering tissues. However, despite these advancements, wide field approaches still face challenges such as background fluorescence and optical aberrations, particularly in deep-tissue imaging. To address these limitations, laser scanning mesoscope

offers an alternative strategy with improved optical sectioning and background suppression.

### Laser scanning imaging

Compared to wide field imaging techniques, most laser scanning methods excite a single point and detect the corresponding signal using a single photodetector, such as a photomultiplier tube (PMT). Typically, confocal microscopy employs a pinhole at the conjugate plane to reject out-of-focus fluorescence signals (Davidovits and Egger 1971). In contrast, multiphoton microscopy

leverages nonlinear optical effects to generate effective excitation only at the specific focal point (Helmchen and Denk 2005; Horton *et al.* 2013).

The imaging speed of confocal and multiphoton microscopy is often limited by the raster scanning process. To overcome this limitation, several scanning strategies have been developed in confocal microscopy to enable multi-point acquisition, such as line-scan confocal (Im *et al.* 2005) and spinning disk confocal (Lchihara *et al.* 1996), which significantly enhance the ability to capture fast cellular dynamics. However, these methods are still limited in imaging performance due to the influence of scattering media, making them typically suitable for transparent or semi-transparent samples such as *C. elegans* and zebrafish. To track the movement of samples over large areas, a low-magnification imaging system is implemented to monitor sample motion and dynamically adjust the stage, ensuring that the imaging target remains within the field of view of the confocal microscope at cellular resolution (Bai *et al.* 2024; Faumont *et al.* 2011; Zhang *et al.* 2021c). This approach effectively expands the field of view of confocal microscopy while maintaining high-resolution imaging.

Compared to confocal microscopy, two-photon microscopy offers superior anti-scattering capabilities, allowing for deeper tissue penetration. Additionally, it induces lower phototoxicity, making it well-suited for mesoscale imaging of organs in many mammalian models. For example, an adaptive brightness modulation system was integrated into a multiphoton microscope, enabling high-quality 3D dynamic imaging of entire lymph nodes (Pinkard *et al.* 2021). The Bessel focus module was incorporated into two-photon imaging, achieving mesoscale volumetric synaptic imaging of the mouse cortex (Lu *et al.* 2020). Several works have miniaturized two-photon microscopes to record neuronal activity in the brains of freely moving rodents (Ziv and Ghosh 2015; Zong *et al.* 2022). Among them, Zong *et al.* optimized the design and developed the MINI2P system, which is capable of recording large-scale, multi-layer neuronal activity, capturing signals from up to 10,000 neurons in the same animal (Zong *et al.* 2022).

Advances in two-photon microscopy are increasingly focused on achieving large FOV, high-speed, multi-depth plane intravital imaging (Demas *et al.* 2021; Sofroniew *et al.* 2016; Stirman *et al.* 2016). To simultaneously expand the imaging depth and FOV while maintaining high spatial and temporal resolution as well as a high signal-to-noise ratio (SNR), it is essential to overcome two main challenges: optimizing the optical system and increasing the speed of sampling

(Ji *et al.* 2016).

Typically, the objective lens and scan engine need to be optimized to increase the field of view while maintaining a high scanning speed and fully utilizing the numerical aperture (NA) of the objective lens, which is crucial to ensure high resolution and SNR. Several works use commercial or customized optical elements to design and set up the two-photon mesoscale imaging system (Ota *et al.* 2021; Tsai *et al.* 2015; Yu *et al.* 2024). For example, Tsai *et al.* developed a serial scanning engine combined with a 0.28 NA commercial objective that recorded across a centimeter-scale FOV (Tsai *et al.* 2015); Ota *et al.* developed FASHIO-2PM, featuring an optimized resonant scanning system and a customized large objective lens with low magnification and high NA (NA = 0.8), enables the recording of 16,000 neurons at 7.5 Hz from a 9 mm<sup>2</sup> contiguous imaging plane (Ota *et al.* 2021). Yu *et al.* developed the Cousa objective, a long-working distance (20 mm) air objective capable of covering an area of over 4 mm<sup>2</sup>, making it highly suitable for intravital mouse brain imaging (Yu *et al.* 2024).

To improve the speed of sampling, several strategies can be employed. First, utilizing faster scanning tools can significantly enhance imaging speed. For instance, inertia-free acousto-optic deflectors (AODs) for beam steering offer an alternative to traditional galvanometer scanners (Bullen *et al.* 1997; Iyer *et al.* 2003) or can be used to only replace resonant galvo (Lechleiter *et al.* 2002) for x-axis scanning, enabling higher lateral scanning speeds and improved temporal resolution. In the axial direction, mechanical methods such as piezo-driven objective lenses are typically slow for fast 3D volume imaging. To overcome this limitation, rapid z-axis focal plane adjustments can be achieved using AODs (Geiller *et al.* 2020; Reddy and Saggau 2005), spatial light modulator (SLM) (Dal Maschio *et al.* 2011) ETL (Grewe *et al.* 2011) or remote scanning mirrors (Botcherby *et al.* 2012).

Second, more effective scanning strategies can be employed to further enhance imaging speed. These approaches focus on optimizing the scanning path or regions of interest (Katona *et al.* 2012; Sofroniew *et al.* 2016; Stirman *et al.* 2016). Instead of the traditional raster scan method, arbitrary line scanning can be optimized to sample a large volume sparsely or targeted to specific regions or cells. For example, a heuristically optimal path was implemented scanning to record activity from thousands of neurons at 8.5 Hz (Sadovskiy *et al.* 2011). Sofroniew *et al.* developed 2pRAM (two-photon random access mesoscope) achieving random access to multiple brain regions and providing diffraction-limited resolution in a cylindrical

volume measuring 5 mm in diameter and 1 mm in depth (Sofroniew *et al.* 2016).

Third, implementing multiple foci to parallelize imaging through multiplexing can increase the imaging speed by a factor proportional to the number of foci when imaging large scale regions or multiple planes (Fig. 4). One approach is to use multiple detectors (Lecoq *et al.* 2014) or a photon array detector (Vaziri and Shank 2010) to record signals simultaneously. Another strategy involves temporally multiplexed foci, where the optical path is adjusted to separate signals temporally from different focal regions between laser pulses (Amir *et al.* 2007; Cheng *et al.* 2011; Clough *et al.* 2021; Demas *et al.* 2021; Stirman *et al.* 2014, 2016; Yu *et al.* 2021). Stirman *et al.* designed temporally multiplexed excitation pathways to simultaneously record two regions, achieving an expanded field of view of approximately 10 mm<sup>2</sup> (Stirman *et al.* 2016) (Fig. 4A). Clough *et al.* developed Quadroscope, which enables the recording of four regions at approximately 10 Hz, covering eight brain regions. Demas *et al.* developed the LBM (light beads mesoscope), splitting the ultrafast pump pulse into 30 copies, which are delayed in time and focused into different depths, enabling the recording of over a million neurons (Demas *et al.* 2021) (Fig. 4C) and providing comprehensive insights into how different brain regions respond to sensory inputs and the neural representations of working memory during behavioral learning, including their stability and causal relationships (Bellafard *et al.* 2024).

The heterogeneity of biological tissues in intravital imaging induces scattering and aberrations, which significantly affect laser scanning imaging. These effects can degrade resolution, reduce the SNR, and decrease excitation efficiency. The distortion of the light is able to be counteracted by adaptive optics (AO) techniques (Ji *et al.* 2010). An adaptive optics system typically consists of a wave front sensing module, which can directly measure aberrations using devices such as a Shack-Hartmann wave front sensor or a pyramid wave front sensor to detect the distorted wave front. Additionally, a wave front correction element, such as a deformable mirror or an SLM, is employed to compensate for the aberrations, thereby achieving optimal focusing for high-quality imaging (Hampson *et al.* 2021). For large FOV correction, Park *et al.* developed a multi-pupil adaptive optics system that maps separate regions of the sample onto different pupil locations (Park *et al.* 2017). Each region undergoes independent AO correction, effectively enabling large-scale, aberration-free intravital imaging across the entire field of view. Similarly, the 2pSAM (two-photon synthetic aperture microscope) achieves fast,

aberration-free 3D imaging with low phototoxicity by utilizing separated apertures to capture images from different angles. These images are then digitally combined through a process known as digital adaptive optics (DAO) (Zhao *et al.* 2023). This approach enables high-speed volumetric imaging with minimal distortion, and reduced phototoxicity, making it well-suited for long-term intravital mesoscale imaging.

In summary, current laser scanning techniques, through the innovative design of objective lenses, scanning engines, scanning strategies, as well as the integration of multiplexing and adaptive optics technologies, have significantly enhanced the performance of intravital mesoscale imaging. Notably, many advanced imaging systems achieve superior performance by combining multiple complementary technologies, leading to substantial improvements in data throughput, SNR, resolution, and overall imaging quality, effectively addressing the challenges of large-scale, high-resolution intravital imaging.

### Computational imaging

With the development of computational techniques, an increasing number of methods can modulate either the illumination or detection paths to achieve coded intravital microscope imaging at the mesoscale. These approaches overcome optical limitations, enabling imaging systems to transmit and reconstruct more information beyond traditional constraints.

One key objective of computational imaging is tomography, as it enables rapid acquisition of 3D spatial information in living samples. Optical coherence tomography (OCT) is widely used for large-scale retinal imaging (Wojtkowski *et al.* 2005) in both animals and humans. Based on low-coherence interferometry, it measures the time delay and intensity of light reflected or scattered from different depths within the sample to obtain high-resolution 3D structures. Fluorescence laminar optical tomography (FLOT) at mesoscale employs laminar illumination to acquire fluorescence projection data from multiple angles (Hillman *et al.* 2007; Yuan *et al.* 2009). Through tomographic reconstruction algorithms, it calculates the 3D fluorescence distribution, enabling applications such as neural activity recording in 3D. Light field imaging techniques (Guo *et al.* 2019; Levoy *et al.* 2006) have been increasingly popular in recent years as a 3D tomographic approach due to their high spatial resolution, tomographic capability, and ability to achieve rapid 3D imaging with low phototoxicity (Orth and Crozier 2013; Scrofani *et al.* 2018; Wagner *et al.* 2019; Xue *et al.* 2020). They are commonly used to

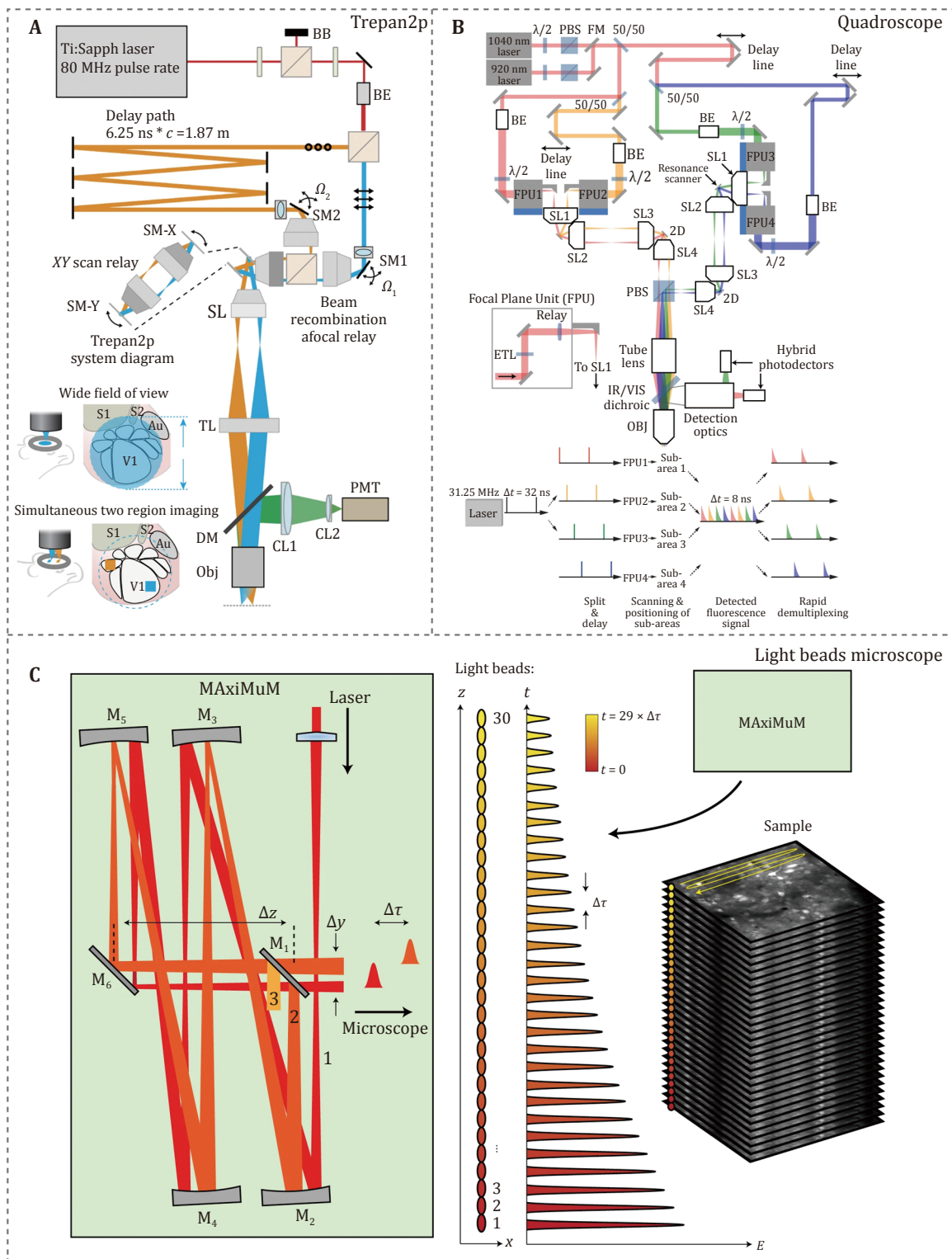


**Fig. 4** **A** Schematic of the Trepan2p system, enabling simultaneous imaging of two regions by temporal multiplexing (Stirman *et al.* 2016). **B** Schematic of the Quaroscope system, enabling simultaneous imaging of four regions by temporal multiplexing (Clough *et al.* 2021). **C** Schematic of light beads microscope system, enabling simultaneous imaging of 30 layers by temporal multiplexing (Demas *et al.* 2021)

capture dynamic processes in living organisms, such as neural activity in zebrafish (Cong *et al.* 2017) and mouse and immune responses in the mouse liver or cortex (Nöbauer *et al.* 2017, 2023; Prevedel *et al.* 2014; Scrofani *et al.* 2018). Microlenses are implemented in the detection path of light field imaging, not only extending the DOF but also capturing both spatial 2D information and angular information simultaneously (Levoy *et al.* 2006; Xiong *et al.* 2021a). Zhang *et al.* developed a precise model for light-field imaging (Zhang *et al.* 2021a), effectively eliminating scattering backgrounds in living tissues, which enables the precise reconstruction of a 3D volume from a single snapshot through post-processing.

Another critical objective is to correct optical aberrations, addressing a century-old challenge in optical design through computational approaches. Traditional optical methods for mesoscale imaging face inherent limitations, primarily due to spatially non-uniform aberrations that arise from the high-throughput optical system design and fabrication process. Additionally, environmental aberrations and scattering induced by tissue heterogeneity further degrade resolution and SNR, while prolonged fluorescence excitation leads to phototoxic effects, limiting long-term high-speed observations. To address these challenges, Eric Betzig's team introduced adaptive lattice light-sheet microscopy (Liu *et al.* 2018), which integrates hardware-based adaptive optics on both the illumination and detection paths. This technique effectively corrects aberrations within a small field of view (FOV) while reducing phototoxicity, enabling long-term imaging. However, this approach inherently compromises 3D imaging speed and the effective imaging FOV.

To further address the challenge of optical aberrations, Wu *et al.* developed a computational imaging framework in 2021 (Wu *et al.* 2021) with detailed practical guidance in 2022 (Lu *et al.* 2022), introducing a high-dimensional spatiotemporal scanning mechanism (Fig. 5A). By leveraging aperture diffraction encoding to impose coherent constraints on an incoherent light field (Fig. 5A), they resolved the trade-off between spatial and angular resolution in conventional light-field imaging methods. This innovation established a novel paradigm of 3D excitation detection, enhancing intravital imaging spatiotemporal resolution by two orders of magnitude while reducing phototoxicity by

three orders of magnitude. The imaging system achieved diffraction-limited resolution at millisecond-level speeds, extending the 3D imaging for intravital observation from the minute scale to six hours.

Further advancing computational imaging, Wu *et al.* proposed digital adaptive optics (DAO) for incoherent light imaging in 2022 (Wu *et al.* 2022). Unlike traditional AO, which relies on SLMs to manipulate wave fronts for aberration correction, DAO estimates aberrations from multi-view data and digitally redistributes light rays in post-processing. This decouples the aberration correction from the imaging process (Cao *et al.* 2024; Guo *et al.* 2024), achieving high-speed, large-scale aberration compensation and opening new avenues for solving the century-old challenge of optical aberrations.

By integrating these two computational imaging innovations, a high-speed, low-phototoxicity mesoscale intravital imaging system (RUSH3D) (Zhang *et al.* 2024a) capable of capturing dynamic 3D imaging across the entire cortical region of live mice at cellular resolution is developed. This system achieves rapid volumetric mesoscale imaging with a FOV of 8 mm × 6 mm × 0.4 mm at 20 Hz, enabling continuous intravital imaging for over 10 h with low phototoxicity (Figs. 5B and 5C). This advancement opens up a new horizon for the study of large-scale intercellular interactions at the mammalian organ level across a long term, which is critical for neural circuit mechanisms, tumor metastasis, and immune responses and may lead to data-driven large-scale biological investigations.

Further improvements were made by integrating a confocal module, which physically suppresses an out-of-focus background (Lu *et al.* 2025). Additionally, multi-angle imaging (Chen *et al.* 2024b; Xiong *et al.* 2021b) and the introduction of spherical aberration phase modulation (Zhang *et al.* 2022) were employed to improve axial resolution and expand the effective axial imaging range. Meanwhile, advancements in 3D reconstruction algorithms, including traditional iterative methods (Broxton *et al.* 2013; Lu *et al.* 2019) and machine learning approaches, have contributed to improved resolution (Liu *et al.* 2023a, 2023b; Lu *et al.* 2023; Wagner *et al.* 2019; Wang *et al.* 2021), artefact reduction (He *et al.* 2021; Zhang *et al.* 2021b; Zhu *et al.* 2022), and enhanced reconstruction speed (Wagner *et al.* 2021; Wang *et al.* 2021), making 3D intravital mesoscale imaging more accessible and efficient.

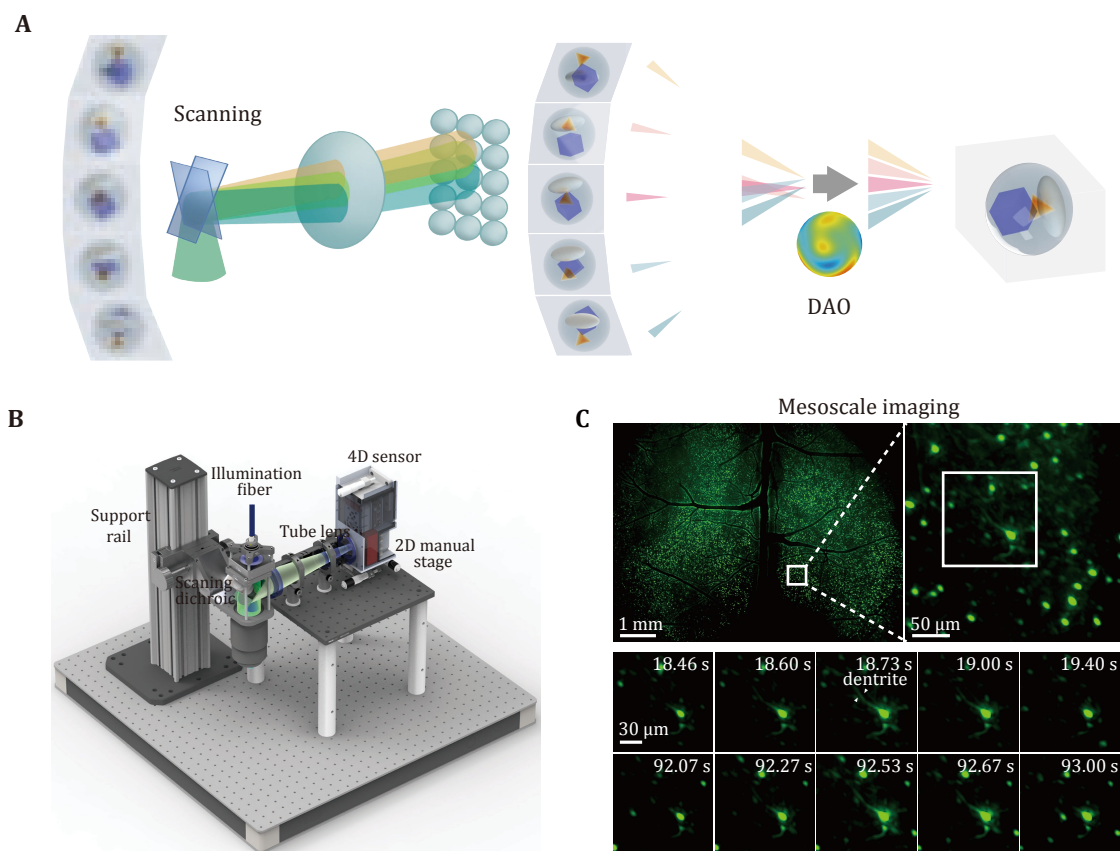


**Fig. 5** **A** Principle of scanning light field imaging mechanism and digital adaptive optics computational framework (Wu *et al.* 2021). **B** Design and assembly of RUSH3D system (Zhang *et al.* 2024a). **C** Mesoscale cortex imaging by RUSH3D system. Top, a perspective of the imaged mouse cortex with thousands of neurons. The FOV is across 8 mm  $\times$  6 mm  $\times$  400  $\mu$ m, with a zoom-in panel. Bottom: Time-lapse visualization of the neuron of interest. As the neuron fires, the dendrite becomes clearly distinguishable (Zhang *et al.* 2024a)

## DISCUSSION AND FUTURE PERSPECTIVES

Intravital mesoscopic imaging has made remarkable progress with the advancement of diverse imaging modalities, enabling high-resolution, large FOV visualization of dynamic biological processes. On this basis, it is essential to address the remaining challenges and explore potential directions for future development.

Although visualization of centimeter-scale tissues is achieved in *ex vivo* imaging, such as mapping an entire rhesus monkey brain (Xu *et al.* 2021) or a whole mouse body (Cai *et al.* 2023), achieving whole-brain neural activity recording intravitaly remains challenging. This limitation arises from constraints in the SBP at video-rate temporal resolution and the restricted imaging depth in living tissues due to scattering and aberrations. Therefore, it is crucial to continue expanding the SBP for larger biological systems and to penetrate deeper into scattering tissues with minimally invasive surgical techniques. Achieving higher SBP

requires not only improvements in optical design to maintain cellular resolution over centimeter-scale fields of view but also innovations in sensor technology and multiplexing strategies. The ability to capture detailed cellular activities across extensive brain regions or whole organs in larger and higher-order animals will profoundly enhance our understanding of complex biological networks (Gilman *et al.* 2017).

As for deeper imaging, future strategies will likely integrate novel modalities such as photoacoustic imaging, which achieves greater penetration depths with high resolution. Alternatively, multiphoton techniques, such as three-photon microscopy (Horton *et al.* 2013), or longer-wavelength fluorophores (Hong *et al.* 2017) in the near-infrared spectrum could be employed, as they offer enhanced tissue penetration, reaching depths of approximately 1 mm below the cortex (Wang *et al.* 2022; Zhao *et al.*, 2023). Additionally, advancements in implantable optics (Paraskevopoulos *et al.* 2022) and non-invasive window (Drew *et al.*

2010; Li *et al.* 2022) or other clearing techniques (Boothe *et al.* 2017; Ou *et al.* 2024) could further reduce tissue disruption, enabling long-term, deep-tissue imaging in living organisms.

A continued focus will be on translating optical bottlenecks into computational solutions. The synergy between optical hardware and computational algorithms will be pivotal in overcoming traditional optical limitations. Computational imaging techniques, such as light field reconstruction (Wagner *et al.* 2021; Wang *et al.* 2021; Wu *et al.* 2021; Zhu *et al.* 2023), compressed sensing (Pavillon and Smith 2016), and deep learning-based deconvolution (Qiao *et al.* 2021), can compensate for aberrations, enhance resolution, and recover high-fidelity 3D structures from mesoscale data. Future imaging systems will likely be co-designed with advanced computational frameworks (Zhang *et al.* 2023b), transforming raw optical signals into rich, interpretable biological information.

Besides, mesoscale imaging generates vast amounts of data, posing significant challenges in storage, processing, and analysis. Developing efficient data handling pipelines that integrate real-time processing and automated imaging enhancement will be challenging and essential (Li *et al.* 2023c). This includes large-scale neural signal extraction (Zhang *et al.* 2023c), high-throughput cell tracking (Arbelle *et al.* 2018), large-field image reconstruction (Zhang *et al.* 2024a) and super-resolution (Foylan 2024), denoising (Chen *et al.* 2024a; Li *et al.* 2021b, 2023a, 2023b; Qiao *et al.* 2024; Zhang *et al.* 2023a), color correction (Zhuang *et al.* 2021), motion drift correction (Pnevmatikakis and Giovannucci 2017), image domain transformation (Li *et al.* 2021a) and mesoscale neuronal data analysis (Cai *et al.* 2022; Xiao *et al.* 2024). Furthermore, the integration of artificial intelligence and machine learning algorithms will accelerate the interpretation of complex datasets, enabling the extraction of meaningful biological insights from terabytes of imaging data.

As mesoscale imaging technologies continue to evolve, their integration with computational methods and innovative imaging modalities will expand the boundaries of intravital biological research. By addressing the challenges of scale, depth, and data complexity, future imaging platforms will offer unprecedented insights into the dynamic processes that govern life at the cellular and biological systems level.

**Acknowledgements** We thank the supports from Beijing Laboratory of Brain and Cognitive Intelligence, Beijing Municipal Education Commission, and Beijing Key Laboratory of Multi-Dimension & Multi-Scale Computational Photography (MMCP).

## Compliance with Ethical Standards

**Conflict of interest** Mingrui Wang, Jiamin Wu, and Qionghai Dai declare that they have no conflict of interests.

**Human and animal rights and informed consent** This article does not contain any studies with human or animal subjects performed by any of the authors.

**Open Access** This article is licensed under a Creative Commons Attribution 4.0 International (CC BY 4.0) License, which permits use, sharing, adaptation, distribution and reproduction in any medium or format, as long as you give appropriate credit to the original author(s) and the source, provide a link to the Creative Commons licence, and indicate if changes were made. The images or other third party material in this article are included in the article's Creative Commons licence, unless indicated otherwise in a credit line to the material. If material is not included in the article's Creative Commons licence and your intended use is not permitted by statutory regulation or exceeds the permitted use, you will need to obtain permission directly from the copyright holder. To view a copy of this licence, visit <http://creativecommons.org/licenses/by/4.0/>.

## References

- Amir W, Carriles R, Hoover EE, Planchon TA, Durfee CG, Squier JA (2007) Simultaneous imaging of multiple focal planes using a two-photon scanning microscope. *Opt Lett* 32(12): 1731–1733
- An H, Huang Y, Zhao Z, Li K, Meng J, Huang X, Tian X, Zhou H, Wu J, Dai Q, Zhang J (2025) Splenic red pulp macrophages eliminate the liver-resistant *Streptococcus pneumoniae* from the blood circulation of mice. *Sci Adv* 11(11): eadq6399. <https://doi.org/10.1126/sciadv.adq6399>
- Arbelle A, Reyes J, Chen J-Y, Lahav G, Raviv TR (2018) A probabilistic approach to joint cell tracking and segmentation in high-throughput microscopy videos. *Med Image Anal* 47: 140–152
- Augustine GJ, Santamaria F, Tanaka K (2003) Local calcium signaling in neurons. *Neuron* 40(2): 331–346
- Bai L, Cong L, Shi Z, Zhao Y, Zhang Y, Lu B, Zhang J, Xiong Z-Q, Xu N, Mu Y, Wang (2024) Volumetric voltage imaging of neuronal populations in the mouse brain by confocal light-field microscopy. *Nat Methods* 21(11): 2160–2170
- Bellafard A, Namvar G, Kao JC, Vaziri A, Golshani P (2024) Volatile working memory representations crystallize with practice. *Nature* 629(8014): 1109–1117
- Bennett AH (1943) The development of the microscope objective. *J Opt Soc Am* 33(3): 123–128
- Berridge MJ (1998) Neuronal calcium signaling. *Neuron* 21(1): 13–26
- Boothe T, Hilbert L, Heide M, Berninger L, Huttner WB, Ziburdaev V, Vastenhouw NL, Myers EW, Drechsel DN, Rink JC (2017) A tunable refractive index matching medium for live imaging cells, tissues and model organisms. *eLife* 6: e27240. <https://doi.org/10.7554/eLife.27240>
- Botcherby EJ, Smith CW, Kohl MM, Débarre D, Booth MJ, Juškaitis R, Paulsen O, Wilson T (2012) Aberration-free three-dimensional multiphoton imaging of neuronal activity at kHz rates. *Proc Natl Acad Sci USA* 109(8): 2919–2924
- Bouchard MB, Voleti V, Mendes CS, Lacefield C, Grueber WB, Mann RS, Bruno RM, Hillman EMC (2015) Swept confocally-aligned

- planar excitation (SCAPE) microscopy for high-speed volumetric imaging of behaving organisms. *Nat Photonics* 9(2): 113–119
- Brady DJ, Hagen N (2009) Multiscale lens design. *Opt Express* 17(13): 10659–10674
- Broxton M, Grosenick L, Yang S, Cohen N, Andalman A, Deisseroth K, Levoy M (2013) Wave optics theory and 3-D deconvolution for the light field microscope. *Opt Express* 21(21): 25418–25439
- Bullen A, Patel SS, Saggau P (1997) High-speed, random-access fluorescence microscopy: I. High-resolution optical recording with voltage-sensitive dyes and ion indicators. *Biophys J* 73(1): 477–491
- Cai R, Kolabas ZI, Pan C, Mai H, Zhao S, Kaltenecker D, Voigt FF, Molbay M, Ohn T-L, Vincke C, Todorov MI, Helmchen F, Van Ginderachter JA, Ertürk A (2023) Whole-mouse clearing and imaging at the cellular level with vDISCO. *Nat Protocols* 18(4): 1197–1242
- Cai Y, Wu J, Dai Q (2022) Review on data analysis methods for mesoscale neural imaging *in vivo*. *Neurophotonics* 9(4): 041407. <https://doi.org/10.1117/1.NPH.9.4.041407>
- Cao Z, Li N, Zhu L, Wu J, Dai Q, Qiao H (2024) Aberration-robust monocular passive depth sensing using a meta-imaging camera. *Light Sci Appl* 13(1): 236. <https://doi.org/10.1038/s41377-024-01609-9>
- Chen X, Qiao C, Jiang T, Liu J, Meng Q, Zeng Y, Chen H, Qiao H, Li D, Wu J (2024a) Self-supervised denoising for multimodal structured illumination microscopy enables long-term super-resolution live-cell imaging. *Photonix* 5(1): 4. <https://doi.org/10.1186/s43074-024-00121-y>
- Chen Y, Wu J, Xiong B, Lu Z, Guo Y, Zhang Y, Fan J, Xiao G, Zhang G, Li X, Wang X, Zhao Z, Dai Q (2024b) High-speed *in toto* 3D imaging with isotropic resolution by scanning light-field tomography. *Optica* 11(10): 1445–1453
- Cheng A, Gonçalves JT, Golshani P, Arisaka K, Portera-Cailliau C (2011) Simultaneous two-photon calcium imaging at different depths with spatiotemporal multiplexing. *Nat Methods* 8(2): 139–142
- Cheng X, Sadegh S, Zilpelwar S, Devor A, Tian L, Boas DA (2020) Comparing the fundamental imaging depth limit of two-photon, three-photon, and non-degenerate two-photon microscopy. *Opt Lett* 45(10): 2934–2937
- Clough M, Chen IA, Park SW, Ahrens AM, Stirman JN, Smith SL, Chen JL (2021) Flexible simultaneous mesoscale two-photon imaging of neural activity at high speeds. *Nat Commun* 12(1): 6638. <https://doi.org/10.1038/s41467-021-26737-3>
- Condeelis JS, Weissleder R (2010) *In vivo* imaging in cancer. *Cold Spring Harbor Perspect Biol* 2(12): a003848. <https://doi.org/10.1101/cshperspect.a003848>
- Cong L, Wang Z, Chai Y, Hang W, Shang C, Yang W, Bai L, Du J, Wang K, Wen Q (2017) Rapid whole brain imaging of neural activity in freely behaving larval zebrafish (*Danio rerio*). *eLife* 6: e28158. <https://doi.org/10.7554/eLife.28158>
- Csencsics E, Sitz B, Schitter G (2020) Integration of control design and system operation of a high performance piezo-actuated fast steering mirror. *IEEE/ASME Trans Mechatron* 25(1): 239–247
- Daetwyler S, Chang B-J, Chen B, Voigt FF, Rajendran D, Zhou F, Fiolka R (2023) Mesoscopic oblique plane microscopy via light-sheet mirroring. *Optica* 10(11): 1571–1581
- Dal Maschio M, De Stasi AM, Benfenati F, Fellin T (2011) Three-dimensional *in vivo* scanning microscopy with inertia-free focus control. *Opt Lett* 36(17): 3503–3505
- Davidovits P, Egger MD (1971) Scanning laser microscope for biological investigations. *Appl Opt* 10(7): 1615–1619
- de Groot A, van den Boom BJG, van Genderen RM, Coppens J, van Veldhuijzen J, Bos J, Hoedemaker H, Negrello M, Willuhn I, De Zeeuw CI, Hoogland TM (2020) NINscope, a versatile miniscope for multi-region circuit investigations. *eLife* 9: e49987. <https://doi.org/10.7554/eLife.49987>
- de Haan K, Rivenson Y, Wu Y, Ozcan A (2020) Deep-learning-based image reconstruction and enhancement in optical microscopy. *Proc IEEE* 108(1): 30–50
- Demas J, Manley J, Tejera F, Barber K, Kim H, Traub FM, Chen B, Vaziri A (2021) High-speed, cortex-wide volumetric recording of neuroactivity at cellular resolution using light beads microscopy. *Nat Methods* 18(9): 1103–1111
- Denk W, Strickler JH, Webb WW (1990) Two-photon laser scanning fluorescence microscopy. *Science* 248(4951): 73–76
- Dong J, Valzania L, Maillard A, Pham T-A, Gigan S, Unser M (2023) Phase retrieval: From computational imaging to machine learning: a tutorial. *IEEE Signal Process Mag* 40(1): 45–57
- Drew PJ, Shih AY, Driscoll JD, Knutsen PM, Blinder P, Davalos D, Akassoglou K, Tsai PS, Kleinfeld D (2010) Chronic optical access through a polished and reinforced thinned skull. *Nat Methods* 7(12): 981–984
- Dunsby C (2008) Optically sectioned imaging by oblique plane microscopy. *Opt Express* 16(25): 20306–20316
- Fan J, Suo J, Wu J, Xie H, Shen Y, Chen F, Wang G, Cao L, Jin G, He Q, Li T, Luan G, Kong L, Zheng Z, Dai Q (2019) Video-rate imaging of biological dynamics at centimetre scale and micrometre resolution. *Nat Photonics* 13(11): 809–816
- Faumont S, Rondeau G, Thiele TR, Lawton KJ, McCormick KE, Sottile M, Griesbeck O, Heckscher ES, Roberts WM, Doe CQ, Lockery SR (2011) An image-free opto-mechanical system for creating virtual environments and imaging neuronal activity in freely moving *Caenorhabditis elegans*. *PLoS One* 6(9): e24666. <https://doi.org/10.1371/journal.pone.0024666>
- Foylan S (2024) Novel optical developments for axial super-resolution microscopy at the mesoscale. PhD thesis, University of Strathclyde
- Geiller T, Vancura B, Terada S, Troullinou E, Chavlis S, Tsagakatakis G, Tsakalides P, Ócsai K, Poirazi P, Rózsa BJ, Losonczy A (2020) Large-scale 3D two-photon imaging of molecularly identified CA1 interneuron dynamics in behaving mice. *Neuron* 108(5): 968–983. e9. <https://doi.org/10.1016/j.neuron.2020.09.013>
- Gilman JP, Medalla M, Luebke JI (2017) Area-specific features of pyramidal neurons—a comparative study in mouse and rhesus monkey. *Cerebral Cortex* 27(3): 2078–2094
- Gonzalez-Figueroa P, Roco JA, Papa I, Villacís LN, Stanley M, Linterman MA, Dent A, Canete PF, Vinuesa CG (2021) Follicular regulatory T cells produce neuritin to regulate B cells. *Cell* 184(7): 1775–1789. e19
- Gottschalk S, Estrada H, Degtyaruk O, Rebling J, Klymenko O, Rosemann M, Razansky D (2015) Short and long-term phototoxicity in cells expressing genetic reporters under nanosecond laser exposure. *Biomaterials* 69: 38–44
- Grandhe VSS, Bandopadhyay A (2023) XY traverse stage for automated microscopy using compliant mechanism. *arXiv*. <https://doi.org/10.48550/arXiv.2311.11022>
- Grewe BF, Voigt FF, van't Hoff M, Helmchen F (2011) Fast two-layer two-photon imaging of neuronal cell populations using an electrically tunable lens. *Biomed Opt Express* 2(7): 2035–2046
- Guo C, Liu W, Hua X, Li H, Jia S (2019) Fourier light-field microscopy. *Opt Express* 27(18): 25573–25594
- Guo C, Blair GJ, Sehgal M, Sanguiliano Jimka FN, Bellafard A, Silva AJ, Golshani P, Basso MA, Blair HT, Aharoni D (2023) Miniscope-LFOV: a large-field-of-view, single-cell-resolution, miniature microscope for wired and wire-free imaging of neural dynamics in freely behaving animals. *Sci Adv* 9(16): eadg3918. <https://doi.org/10.1126/sciadv.adg3918>

- Guo Y, Hao Y, Wan S, Zhang H, Zhu L, Zhang Y, Wu J, Dai Q, Fang L (2024) Direct observation of atmospheric turbulence with a video-rate wide-field wavefront sensor. *Nat Photonics* 18(9): 935–943
- Gustafsson MGL (2000) Surpassing the lateral resolution limit by a factor of two using structured illumination microscopy. *J Microsc* 198(2): 82–87
- Gustafsson MGL, Shao L, Carlton PM, Wang CJR, Golubovskaya IN, Cande WZ, Agard DA, Sedat JW (2008) Three-dimensional resolution doubling in wide-field fluorescence microscopy by structured illumination. *Biophys J* 94(12): 4957–4970
- Hampson KM, Turcotte R, Miller DT, Kurokawa K, Males JR, Ji N, Booth MJ (2021) Adaptive optics for high-resolution imaging. *Nat Rev Methods Primers* 1(1): 68. <https://doi.org/10.1038/s43586-021-00066-7>
- He J, Cai Y, Wu J, Dai Q (2021) Spatial-temporal low-rank prior for low-light volumetric fluorescence imaging. *Opt Express* 29(25): 40721–40733
- Helmchen F, Denk W (2005) Deep tissue two-photon microscopy. *Nat Methods* 2(12): 932–940
- Hillman EMC, Bernus O, Pease E, Bouchard MB, Pertsov A (2007) Depth-resolved optical imaging of transmural electrical propagation in perfused heart. *Opt Express* 15(26): 17827–17841
- Hoffmann M, Judkewitz B (2019) Diffractive oblique plane microscopy. *Optica* 6(9): 1166–1170
- Hoffmann M, Henninger J, Veith J, Richter L, Judkewitz B (2023) Blazed oblique plane microscopy reveals scale-invariant inference of brain-wide population activity. *Nat Commun* 14(1): 8019. <https://doi.org/10.1038/s41467-023-43741-x>
- Holtmaat A, Bonhoeffer T, Chow DK, Chuckowree J, De Paola V, Hofer SB, Hübener M, Keck T, Knott G, Lee WCA, Mostany R, Mrsic-Flogel TD, Nedivi E, Portera-Cailliau C, Svoboda K, Trachtenberg JT, Willbrecht L (2009) Long-term, high-resolution imaging in the mouse neocortex through a chronic cranial window. *Nat Protoc* 4(8): 1128–1144
- Hong GS, Antaris AL, Dai HJ (2017) Near-infrared fluorophores for biomedical imaging. *Nat Biomed Eng* 1(1): 0010. <https://doi.org/10.1038/s41551-016-0010>
- Hopt A, Neher E (2001) Highly nonlinear photodamage in two-photon fluorescence microscopy. *Biophys J* 80(4): 2029–2036
- Horton NG, Wang K, Kobat D, Clark CG, Wise FW, Schaffer CB, Xu C (2013) *In vivo* three-photon microscopy of subcortical structures within an intact mouse brain. *Nat Photonics* 7(3): 205–209
- Huisken J, Swoger J, Del Bene F, Wittbrodt J, Stelzer EHK (2004) Optical sectioning deep inside live embryos by selective plane illumination microscopy. *Science* 305(5686): 1007–1009
- Im K-B, Han S, Park H, Kim D, Kim B-M (2005) Simple high-speed confocal line-scanning microscope. *Opt Express* 13(13): 5151–5156
- Iyer V, Losavio BE, Saggau P (2003) Compensation of spatial and temporal dispersion for acousto-optic multiphoton laser-scanning microscopy. *J Biomed Opt* 8(3): 460–471
- Ji N, Milkie DE, Betzig E (2010) Adaptive optics via pupil segmentation for high-resolution imaging in biological tissues. *Nat Methods* 7(2): 141–147
- Ji N, Freeman J, Smith SL (2016) Technologies for imaging neural activity in large volumes. *Nat Neurosci* 19(9): 1154–1164
- Katona G, Szalay G, Maák P, Kaszás A, Veress M, Hillier D, Chiovini B, Vizi ES, Roska B, Rózsa B (2012) Fast two-photon *in vivo* imaging with three-dimensional random-access scanning in large tissue volumes. *Nat Methods* 9(2): 201–208
- Khanna C, Hunter K (2005) Modeling metastasis *in vivo*. *Carcinogenesis* 26(3): 513–523
- Kim TH, Zhang Y, Lecoq J, Jung JC, Li J, Zeng H, Niell CM, Schnitzer MJ (2016) Long-term optical access to an estimated one million neurons in the live mouse cortex. *Cell Rep* 17(12): 3385–3394
- Klonis N, Rug M, Harper I, Wickham M, Cowman A, Tilley L (2002) Fluorescence photobleaching analysis for the study of cellular dynamics. *Eur Biophys J* 31(1): 36–51
- Kumar M, Kishore S, Nasenbeny J, McLean DL, Kozorovitskiy Y (2018) Integrated one-and two-photon scanned oblique plane illumination (SOPi) microscopy for rapid volumetric imaging. *Opt Express* 26(10): 13027–13041
- Kumar M, Kozorovitskiy Y (2019) Tilt-invariant scanned oblique plane illumination microscopy for large-scale volumetric imaging. *Opt Lett* 44(7): 1706–1709
- Lchihara A, Tanaami T, Lsozaki K, Sugiyama Y, Kosugi Y, Mikuriya K, Abe M, Uemura L (1996) High-speed confocal fluorescence microscopy using a nipkow scanner with microlenses for 3-D imaging of single fluorescent molecule in real time. *Bioimages* 4(2): 57–62
- Lechleiter JD, Lin D-T, Sieneart I (2002) Multi-photon laser scanning microscopy using an acoustic optical deflector. *Biophys J* 83(4): 2292–2299
- Lecoq J, Savall J, Vučinić D, Grewe BF, Kim H, Li JZ, Kitch LJ, Schnitzer MJ (2014) Visualizing mammalian brain area interactions by dual-axis two-photon calcium imaging. *Nat Neurosci* 17(12): 1825–1829
- Lerman YV, Kim M (2015) Neutrophil migration under normal and sepsis conditions. *Cardiovasc Haematol Disord Drug Targets* 15(1): 19–28
- Levoy M, Ng R, Adams A, Footer M, Horowitz M (2006) Light field microscopy. In: *Proceedings of the ACM SIGGRAPH 2006 papers*. Boston: ACM, pp 924–934
- Li D, Hu Z, Zhang H, Yang Q, Zhu L, Liu Y, Yu T, Zhu J, Wu J, He J, Fei P, Xi W, Qian J, Zhu D (2022) A Through-Intact-Skull (TIS) chronic window technique for cortical structure and function observation in mice. *eLight* 2(1): 15. <https://doi.org/10.1186/s43593-022-00022-2>
- Li X, Zhang G, Qiao H, Bao F, Deng Y, Wu J, He Y, Yun J, Lin X, Xie H, Wang H, Dai Q (2021a) Unsupervised content-preserving transformation for optical microscopy. *Light: Sci Appl* 10(1): 44. <https://doi.org/10.1038/s41377-021-00484-y>
- Li X, Zhang G, Wu J, Zhang Y, Zhao Z, Lin X, Qiao H, Xie H, Wang H, Fang L, Dai Q (2021b) Reinforcing neuron extraction and spike inference in calcium imaging using deep self-supervised denoising. *Nat Methods* 18(11): 1395–1400
- Li X, Hu X, Chen X, Fan J, Zhao Z, Wu J, Wang H, Dai Q (2023a) Spatial redundancy transformer for self-supervised fluorescence image denoising. *Nat Comput Sci* 3(12): 1067–1080
- Li X, Li Y, Zhou Y, Wu J, Zhao Z, Fan J, Deng F, Wu Z, Xiao G, He J, Zhang Y, Zhang G, Hu X, Chen X, Zhang Y, Qiao H, Xie H, Li Y, Wang H, Fang L, Dai Q (2023b) Real-time denoising enables high-sensitivity fluorescence time-lapse imaging beyond the shot-noise limit. *Nat Biotechnol* 41(2): 282–292
- Li X, Zhang Y, Wu J, Dai Q (2023c) Challenges and opportunities in bioimage analysis. *Nat Methods* 20(7): 958–961
- Liu G, Yue H, Wu J, Yang J (2023a) Intra-inter view interaction network for light field image super-resolution. *IEEE Trans Multimedia* 25: 256–266
- Liu G, Yue H, Wu J, Yang J (2023b) Efficient light field angular super-resolution with sub-aperture feature learning and macro-pixel upsampling. *IEEE Trans Multimedia* 25: 6588–6600
- Liu T-L, Upadhyayula S, Milkie DE, Singh V, Wang K, Swinburne IA, Mosaliganti KR, Collins ZM, Hiscock TW, Shea J, Kohrman AQ, Medwig TN, Dambournet D, Forster R, Cuniff B, Ruan Y, Yashiro H, Scholpp S, Meyerowitz EM, Hockemeyer D, Drubin

- DG, Martin BL, Matus DQ, Koyama M, Megason SG, Kirchhausen T, Betzig E (2018) Observing the cell in its native state: imaging subcellular dynamics in multicellular organisms. *Science* 360(6386): eaaq1392. <https://doi.org/10.1126/science.aaq1392>
- Lohmann AW (1989) Scaling laws for lens systems. *Appl Opt* 28(23): 4996–4998
- Lohmann AW, Dorsch RG, Mendlovic D, Zalevsky Z, Ferreira C (1996) Space-bandwidth product of optical signals and systems. *J Opt Soc Am A* 13(3): 470–473
- Lu R, Liang Y, Meng G, Zhou P, Svoboda K, Paninski L, Ji N (2020) Rapid mesoscale volumetric imaging of neural activity with synaptic resolution. *Nat Methods* 17(3): 291–294
- Lu Z, Wu J, Qiao H, Zhou Y, Yan T, Zhou Z, Zhang X, Fan J, Dai Q (2019) Phase-space deconvolution for light field microscopy. *Opt Express* 27(13): 18131–18145
- Lu Z, Cai Y, Nie Y, Yang Y, Wu J, Dai Q (2022) A practical guide to scanning light-field microscopy with digital adaptive optics. *Nat Protocols* 17(9): 1953–1979
- Lu Z, Liu Y, Jin M, Luo X, Yue H, Wang Z, Zuo S, Zeng Y, Fan J, Pang Y, Wu J, Yang J, Dai Q (2023) Virtual-scanning light-field microscopy for robust snapshot high-resolution volumetric imaging. *Nat Methods* 20(5): 735–746
- Lu Z, Zuo S, Shi M, Fan J, Xie J, Xiao G, Yu L, Wu J, Dai Q (2025) Long-term intravital subcellular imaging with confocal scanning light-field microscopy. *Nat Biotechnol* 43(4): 569–580
- MacLennan IC (1994) Germinal centers. *Annu Rev Immunol* 12: 117–139
- Magidson V, Khodjakov A (2013) Circumventing photodamage in live-cell microscopy. *Methods Cell Biol* 114: 545–560
- Mait JN, Euliss GW, Athale RA (2018) Computational imaging. *Adv Opt Photonics* 10(2): 409–483
- McConnell G, Trägårdh J, Amor R, Dempster J, Reid E, Amos WB (2016) A novel optical microscope for imaging large embryos and tissue volumes with sub-cellular resolution throughout. *eLife* 5: e18659. <https://doi.org/10.7554/eLife.18659>
- Mendlovic D, Lohmann AW, Zalevsky Z (1997) Space-bandwidth product adaptation and its application to superresolution: examples. *J Opt Soc Am A* 14(3): 563–567
- Minsky M (1988) Memoir on inventing the confocal scanning microscope. *Scanning* 10(4): 128–138
- Negrean A, Mansvelder HD (2014) Optimal lens design and use in laser-scanning microscopy. *Biomed Opt Express* 5(5): 1588–1609
- Nikolenko V, Watson BO, Araya R, Woodruff A, Peterka DS, Yuste R (2008) SLM microscopy: scanless two-photon imaging and photostimulation with spatial light modulators. *Front Neural Circuits* 2: 393. <https://doi.org/10.3389/neuro.04.005.2008>
- Nöbauer T, Skocek O, Pernía-Andrade AJ, Weilguny L, Traub FM, Molodtsov MI, Vaziri A (2017) Video rate volumetric Ca<sup>2+</sup> imaging across cortex using seeded iterative demixing (SID) microscopy. *Nat Methods* 14(8): 811–818
- Nöbauer T, Zhang Y, Kim H, Vaziri A (2023) Mesoscale volumetric light-field (MesoLF) imaging of neuroactivity across cortical areas at 18 Hz. *Nat Methods* 20(4): 600–609
- Oleksievets N, Mathew C, Thiele JC, Gallea JI, Nevskiy O, Gregor I, Weber A, Tsukanov R, Enderlein J (2022) Single-molecule fluorescence lifetime imaging using wide-field and confocal-laser scanning microscopy: a comparative analysis. *Nano Lett* 22(15): 6454–6461
- Orth A, Crozier K (2013) Gigapixel fluorescence microscopy with a water immersion microlens array. *Opt Express* 21(2): 2361–2368
- Ota K, Oisi Y, Suzuki T, Ikeda M, Ito Y, Ito T, Uwamori H, Kobayashi K, Kobayashi M, Odagawa M, Matsubara C, Kuroiwa Y, Horikoshi M, Matsushita J, Hioki H, Ohkura M, Nakai J, Oizumi M, Miyawaki A, Aonishi T, Ode T, Murayama M (2021) Fast, cell-resolution, contiguous-wide two-photon imaging to reveal functional network architectures across multi-modal cortical areas. *Neuron* 109(11): 1810–1824. e9
- Otomo K, Hibi T, Murata T, Watanabe H, Kawakami R, Nakayama H, Hasebe M, Nemoto T (2015) Multi-point scanning two-photon excitation microscopy by utilizing a high-peak-power 1042-nm laser. *Anal Sci* 31(4): 307–313
- Otsu Y, Bormuth V, Wong J, Mathieu B, Dugué GP, Feltz A, Dieudonné S (2008) Optical monitoring of neuronal activity at high frame rate with a digital random-access multiphoton (RAMP) microscope. *J Neurosci Methods* 173(2): 259–270
- Ou Z, Duh Y-S, Rommelfanger NJ, Keck CHC, Jiang S, Brinson Jr K, Zhao S, Schmidt EL, Wu X, Yang F, Cai B, Cui H, Qi W, Wu S, Tantry A, Roth R, Ding J, Chen X, Kaltschmidt JA, Brongersma ML, Hong G (2024) Achieving optical transparency in live animals with absorbing molecules. *Science* 385(6713): eadm6869. <https://doi.org/10.1126/science.adm6869>
- Paraskevopoulos A, Maggiorelli F, Albani M, Maci S (2022) Radial GRIN lenses based on the solution of a regularized ray congruence equation. *IEEE Trans Antennas Propag* 70(2): 888–899
- Park J, Brady DJ, Zheng G, Tian L, Gao L (2021) Review of bio-optical imaging systems with a high space-bandwidth product. *Adv Photonics* 3(4): 044001. <https://doi.org/10.1117/1.ap.3.4.044001>
- Park J-H, Kong L, Zhou Y, Cui M (2017) Large-field-of-view imaging by multi-pupil adaptive optics. *Nat Methods* 14(6): 581–583
- Pavillon N, Smith NI (2016) Compressed sensing laser scanning microscopy. *Opt Express* 24(26): 30038–30052
- Peterka DS, Takahashi H, Yuste R (2011) Imaging voltage in neurons. *Neuron* 69(1): 9–21
- Pinkard H, Baghdassarian H, Mujal A, Roberts E, Hu KH, Friedman DH, Malenica I, Shagam T, Fries A, Corbin K, Krummel MF, Waller L (2021) Learned adaptive multiphoton illumination microscopy for large-scale immune response imaging. *Nat Commun* 12(1): 1916. <https://doi.org/10.1038/s41467-021-22246-5>
- Pittet MJ, Weissleder R (2011) Intravital imaging. *Cell* 147(5): 983–991
- Pnevmatikakis EA, Giovannucci A (2017) NoRMCorre: an online algorithm for piecewise rigid motion correction of calcium imaging data. *J Neurosci Methods* 291: 83–94
- Potsaid B, Bellouard Y, Wen JT (2005) Adaptive Scanning Optical Microscope (ASOM): a multidisciplinary optical microscope design for large field of view and high resolution imaging. *Opt Express* 13(17): 6504–6518
- Prasher DC (1995) Using GFP to see the light. *Trends Genet* 11(8): 320–323
- Prevedel R, Yoon YG, Hoffmann M, Pak N, Wetzstein G, Kato S, Schrödel T, Raskar R, Zimmer M, Boyden ES, Vaziri A (2014) Simultaneous whole-animal 3D imaging of neuronal activity using light-field microscopy. *Nat Methods* 11(7): 727–730
- Qiao C, Li D, Guo Y, Liu C, Jiang T, Dai Q, Li D (2021) Evaluation and development of deep neural networks for image super-resolution in optical microscopy. *Nat Methods* 18(2): 194–202
- Qiao C, Zeng Y, Meng Q, Chen X, Chen H, Jiang T, Wei R, Guo J, Fu W, Lu H, Li D, Wang Y, Qiao H, Wu J, Li D, Dai Q (2024) Zero-shot learning enables instant denoising and super-resolution in optical fluorescence microscopy. *Nat Commun* 15(1): 4180. <https://doi.org/10.1038/s41467-024-48575-9>
- Reddy GD, Saggau P (2005) Fast three-dimensional laser scanning scheme using acousto-optic deflectors. *J Biomed Opt* 10(6): 064038. <https://doi.org/10.1117/1.2141504>

- Ren Y-X, Wu J, Lai QTK, Lai HM, Siu DMD, Wu W, Wong KKY, Tsia KK (2020) Parallelized volumetric fluorescence microscopy with a reconfigurable coded incoherent light-sheet array. *Light: Sci Appl* 9(1): 8. <https://doi.org/10.1038/s41377-020-0245-8>
- Rivenson Y, Göröcs Z, Günaydin H, Zhang Y, Wang H, Ozcan A (2017) Deep learning microscopy. *Optica* 4(11): 1437–1443
- Rynes ML, Surinach DA, Linn S, Laroque M, Rajendran V, Dominguez J, Hadjistamoulou O, Navabi ZS, Ghanbari L, Johnson GW, Nazari M, Mohajerani MH, Kodandaramaiah SB (2021) Miniaturized head-mounted microscope for whole-cortex mesoscale imaging in freely behaving mice. *Nat Methods* 18(4): 417–425
- Sadovsky AJ, Kruskal PB, Kimmel JM, Ostmeier J, Neubauer FB, MacLean JN (2011) Heuristically optimal path scanning for high-speed multiphoton circuit imaging. *J Neurophysiol* 106(3): 1591–1598
- Salvermoser M, Begandt D, Alon R, Walzog B (2018) Nuclear deformation during neutrophil migration at sites of inflammation. *Front Immunol* 9: 2680. <https://doi.org/10.3389/fimmu.2018.02680>
- Schneckenburger H, Richter V (2021) Laser scanning versus wide-field—choosing the appropriate microscope in life sciences. *Appl Sci* 11(2): 733. <https://doi.org/10.3390/app11020733>
- Schwertner M, Booth MJ, Neil MAA, Wilson T (2004) Measurement of specimen-induced aberrations of biological samples using phase stepping interferometry. *J Microsc* 213(1): 11–19
- Scrofani G, Sola-Pikabea J, Llavador A, Sanchez-Ortiga E, Barreiro JC, Saavedra G, Garcia-Sucerquia J, Martínez-Corral M (2018) FIMic: design for ultimate 3D-integral microscopy of *in-vivo* biological samples. *Biomed Opt Express* 9(1): 335–346
- Shao W, Chang M, Emmerich K, Kanold PO, Mumm JS, Yi J (2022) Mesoscopic oblique plane microscopy with a diffractive light-sheet for large-scale 4D cellular resolution imaging. *Optica* 9(12): 1374–1385
- Sheppard CJR, Choudhury A (1977) Image formation in the scanning microscope. *Opt Acta: Int J Opt* 24(10): 1051–1073
- Shi R, Chen X, Deng J, Liang J, Fan K, Zhou F, Tang P, Zhang L, Kong L (2024) Random-access wide-field mesoscopy for centimetre-scale imaging of biodynamics with subcellular resolution. *Nat Photonics* 18(7): 721–730
- Shimomura O, Johnson FH, Saiga Y (1962) Extraction, purification and properties of aequorin, a bioluminescent protein from the luminous hydromedusa, *Aequorea*. *J Cell Comp Physiol* 59(3): 223–239
- Sofroniew NJ, Flickinger D, King J, Svoboda K (2016) A large field of view two-photon mesoscope with subcellular resolution for *in vivo* imaging. *eLife* 5: e14472. <https://doi.org/10.7554/eLife.14472>
- Stirman JN, Smith IT, Kudenov MW, Smith SL (2014) Wide field-of-view, twin-region two-photon imaging across extended cortical networks. *bioRxiv*. <https://doi.org/10.1101/011320>
- Stirman JN, Smith IT, Kudenov MW, Smith SL (2016) Wide field-of-view, multi-region, two-photon imaging of neuronal activity in the mammalian brain. *Nat Biotechnol* 34(8): 857–862
- Swedlow JR, Hu K, Andrews PD, Roos DS, Murray JM (2002) Measuring tubulin content in *Toxoplasma gondii*: a comparison of laser-scanning confocal and wide-field fluorescence microscopy. *Proc Natl Acad Sci USA* 99(4): 2014–2019
- Tomer R, Lovett-Barron M, Kauvar I, Andalman A, Burns VM, Sankaran S, Grosenick L, Broxton M, Yang S, Deisseroth K (2015) SPED light sheet microscopy: fast mapping of biological system structure and function. *Cell* 163(7): 1796–1806
- Tsai PS, Mateo C, Field JJ, Schaffer CB, Anderson ME, Kleinfeld D (2015) Ultra-large field-of-view two-photon microscopy. *Opt Express* 23(11): 13833–13847
- Vaziri A, Shank CV (2010) Ultrafast widefield optical sectioning microscopy by multifocal temporal focusing. *Opt Express* 18(19): 19645–19655
- Victoria GD, Schwickert TA, Fooksman DR, Kamphorst AO, Meyer-Hermann M, Dustin ML, Nussenzweig MC (2010) Germinal center dynamics revealed by multiphoton microscopy with a photoactivatable fluorescent reporter. *Cell* 143(4): 592–605
- Voleti V, Patel KB, Li W, Perez Campos C, Bharadwaj S, Yu H, Ford C, Casper MJ, Yan RW, Liang W, Wen C, Kimura KD, Targoff KL, Hillman EMC (2019) Real-time volumetric microscopy of *in vivo* dynamics and large-scale samples with SCAPE 2.0. *Nat Methods* 16(10): 1054–1062
- Wagner N, Norlin N, Gierten J, de Medeiros G, Balázs B, Wittbrodt J, Hufnagel L, Prevedel R (2019) Instantaneous isotropic volumetric imaging of fast biological processes. *Nat Methods* 16(6): 497–500
- Wagner N, Beuttenmueller F, Norlin N, Gierten J, Boffi JC, Wittbrodt J, Weigert M, Hufnagel L, Prevedel R, Kreshuk A (2021) Deep learning-enhanced light-field imaging with continuous validation. *Nat Methods* 18(5): 557–563
- Wang F, Ren F, Ma Z, Qu L, Gourgues R, Xu C, Baghdasaryan A, Li J, Zadeh IE, Los JWN, Fognini A, Qin-Dregely J, Dai H (2022) *In vivo* non-invasive confocal fluorescence imaging beyond 1,700 nm using superconducting nanowire single-photon detectors. *Nat Nanotechnol* 17(6): 653–660
- Wang H, Rivenson Y, Jin Y, Wei Z, Gao R, Günaydin H, Bentolila LA, Kural C, Ozcan A (2019) Deep learning enables cross-modality super-resolution in fluorescence microscopy. *Nat Methods* 16(1): 103–110
- Wang Y, You L, Tan K, Li M, Zou J, Zhao Z, Hu W, Li T, Xie F, Li C, Yuan R, Ding K, Cao L, Xin F, Shang C, Liu M, Gao Y, Wei L, You Z, Gao X, Xiong W, Cao P, Luo M, Chen F, Li K, Wu J, Hong B, Yuan K (2023) A common thalamic hub for general and defensive arousal control. *Neuron* 111(20): 3270–3287. e8
- Wang Z, Zhu L, Zhang H, Li G, Yi C, Li Y, Yang Y, Ding Y, Zhen M, Gao S, Hsiai TK, Fei P (2021) Real-time volumetric reconstruction of biological dynamics with light-field microscopy and deep learning. *Nat Methods* 18(5): 551–556
- Weigert M, Schmidt U, Boothe T, Müller A, Dibrov A, Jain A, Wilhelm B, Schmidt D, Broaddus C, Culley S, Rocha-Martins M, Segovia-Miranda F, Norden C, Henriques R, Zerial M, Solimena M, Rink J, Tomancak P, Royer L, Jug F, Myers EW (2018) Content-aware image restoration: pushing the limits of fluorescence microscopy. *Nat Methods* 15(12): 1090–1097
- Welford WT (2017) *Aberrations of optical systems*. New York: Routledge
- Wen C, Ren M, Feng F, Chen W, Chen S-C (2019) Compressive sensing for fast 3-D and random-access two-photon microscopy. *Opt Lett* 44(17): 4343–4346
- Werley CA, Chien M-P, Cohen AE (2017) Ultrawidefield microscope for high-speed fluorescence imaging and targeted optogenetic stimulation. *Biomed Opt Express* 8(12): 5794–5813
- Wojtkowski M, Srinivasan V, Fujimoto JG, Ko T, Schuman JS, Kowalczyk A, Duker JS (2005) Three-dimensional retinal imaging with high-speed ultrahigh-resolution optical coherence tomography. *Ophthalmology* 112(10): 1734–1746
- Wu J, Lu Z, Jiang D, Guo Y, Qiao H, Zhang Y, Zhu T, Cai Y, Zhang X, Zhanghao K, Xie H, Yan T, Zhang G, Li X, Jiang Z, Lin X, Fang L, Zhou B, Xi P, Fan J, Yu L, Dai Q (2021) Iterative tomography with digital adaptive optics permits hour-long intravital observation of 3D subcellular dynamics at millisecond scale. *Cell* 184(12): 3318–3332. e17
- Wu J, Guo Y, Deng C, Zhang A, Qiao H, Lu Z, Xie J, Fang L, Dai Q (2022) An integrated imaging sensor for aberration-corrected 3D photography. *Nature* 612(7938): 62–71

- Xiao G, Cai Y, Zhang Y, Xie J, Wu L, Xie H, Wu J, Dai Q (2024) Mesoscale neuronal granular trial variability *in vivo* illustrated by nonlinear recurrent network *in silico*. *Nat Commun* 15(1): 9894. <https://doi.org/10.1038/s41467-024-54346-3>
- Xie H, Han X, Xiao G, Xu H, Zhang Y, Zhang G, Li Q, He J, Zhu D, Yu X, Dai Q (2024) Multifocal fluorescence video-rate imaging of centimetre-wide arbitrarily shaped brain surfaces at micrometric resolution. *Nat Biomed Eng* 8(6): 740–753
- Xiong B, Li X, Zhou Y, Wang L, Wu J, Dai Q (2021a) Snapshot partially coherent diffraction tomography. *Phys Rev Appl* 15(4): 044048. <https://doi.org/10.1103/PhysRevApplied.15.044048>
- Xiong B, Zhu T, Xiang Y, Li X, Yu J, Jiang Z, Niu Y, Jiang D, Zhang X, Fang L, Wu J, Dai Q (2021b) Mirror-enhanced scanning light-field microscopy for long-term high-speed 3D imaging with isotropic resolution. *Light Sci Appl* 10(1): 227. <https://doi.org/10.1038/s41377-021-00665-9>
- Xu F, Shen Y, Ding L, Yang C-Y, Tan H, Wang H, Zhu Q, Xu R, Wu F, Xiao Y, Xu C, Li Q, Su P, Zhang L, Dong H-W, Desimone R, Xu F, Hu X, Lau P-M, Bi G-Q (2021) High-throughput mapping of a whole rhesus monkey brain at micrometer resolution. *Nat Biotechnol* 39(12): 1521–1528
- Xu Q, Zhao W, Yan M, Mei H (2022) Neutrophil reverse migration. *J Inflamm* 19(1): 22. <https://doi.org/10.1186/s12950-022-00320-z>
- Xue Y, Davison IG, Boas DA, Tian L (2020) Single-shot 3D wide-field fluorescence imaging with a computational miniature mesoscope. *Sci Adv* 6(43): eabb7508. <https://doi.org/10.1126/sciadv.abb7508>
- Yan B, Wang Z, Parker AL, Lai Y-K, John Thomas P, Yue L, Monks JN (2017) Superlensing microscope objective lens. *Appl Opt* 56(11): 3142–3147
- Yang G, Pan F, Parkhurst CN, Grutzendler J, Gan WB (2010) Thinned-skull cranial window technique for long-term imaging of the cortex in live mice. *Nat Protoc* 5(2): 201–208
- Yang W, Yuste R (2018) Holographic imaging and photostimulation of neural activity. *Curr Opin Neurobiol* 50: 211–221
- Yu C-H, Stirman JN, Yu Y, Hira R, Smith SL (2021) Diesel2p mesoscope with dual independent scan engines for flexible capture of dynamics in distributed neural circuitry. *Nat Commun* 12(1): 6639. <https://doi.org/10.1038/s41467-021-26736-4>
- Yu C-H, Yu Y, Adsit LM, Chang JT, Barchini J, Moberly AH, Benisty H, Kim J, Young BK, Heng K, Farinella DM, Leikvoll A, Pavan R, Vistein R, Nanfeto BR, Hildebrand DGC, Otero-Coronel S, Vaziri A, Goldberg JL, Ricci AJ, Fitzpatrick D, Cardin JA, Higley MJ, Smith GB, Kara P, Nielsen KJ, Smith IT, Smith SL (2024) The Cousa objective: a long-working distance air objective for multiphoton imaging *in vivo*. *Nat Methods* 21(1): 132–141
- Yuan B, Burgess SA, Iranmahboob A, Bouchard MB, Lehrer N, Bordier C, Hillman EMC (2009) A system for high-resolution depth-resolved optical imaging of fluorescence and absorption contrast. *Rev Sci Instrum* 80(4): 043706. <https://doi.org/10.1063/1.3117204>
- Zhang G, Li X, Zhang Y, Han X, Li X, Yu J, Liu B, Wu J, Yu L, Dai Q (2023a) Bio-friendly long-term subcellular dynamic recording by self-supervised image enhancement microscopy. *Nat Methods* 20(12): 1957–1970
- Zhang Y, Lu Z, Wu J, Lin X, Jiang D, Cai Y, Xie J, Wang Y, Zhu T, Ji X, Dai Q (2021a) Computational optical sectioning with an incoherent multiscale scattering model for light-field microscopy. *Nat Commun* 12(1): 6391. <https://doi.org/10.1038/s41467-021-26730-w>
- Zhang Y, Wang Y, Wang M, Guo Y, Li X, Chen Y, Lu Z, Wu J, Ji X, Dai Q (2022) Multi-focus light-field microscopy for high-speed large-volume imaging. *Photonix* 3(1): 30. <https://doi.org/10.1186/s43074-022-00076-y>
- Zhang Y, Xiong B, Zhang Y, Lu Z, Wu J, Dai Q (2021b) DiLFM: an artifact-suppressed and noise-robust light-field microscopy through dictionary learning. *Light Sci Appl* 10(1): 152. <https://doi.org/10.1038/s41377-021-00587-6>
- Zhang Y, Song X, Xie J, Hu J, Chen J, Li X, Zhang H, Zhou Q, Yuan L, Kong C, Shen Y, Wu J, Fang L, Dai Q (2023b) Large depth-of-field ultra-compact microscope by progressive optimization and deep learning. *Nat Commun* 14(1): 4118. <https://doi.org/10.1038/s41467-023-39860-0>
- Zhang Y, Zhang G, Han X, Wu J, Li Z, Li X, Xiao G, Xie H, Fang L, Dai Q (2023c) Rapid detection of neurons in widefield calcium imaging datasets after training with synthetic data. *Nat Methods* 20(5): 747–754
- Zhang Y, Wang M, Zhu Q, Guo Y, Liu B, Li J, Yao X, Kong C, Zhang Y, Huang Y, Qi H, Wu J, Guo Z, Dai Q (2024a) Long-term mesoscale imaging of 3D intercellular dynamics across a mammalian organ. *Cell* 187(21): 6104–6122. e25
- Zhang Y, Yuan L, Zhu Q, Wu J, Nöbauer T, Zhang R, Xiao G, Wang M, Xie H, Guo ZC, Dai Q, Vaziri A (2024b) A miniaturized mesoscope for the large-scale single-neuron-resolved imaging of neuronal activity in freely behaving mice. *Nat Biomed Eng* 8(6): 754–774
- Zhang Z, Bai L, Cong L, Yu P, Zhang T, Shi W, Li F, Du J, Wang K (2021c) Imaging volumetric dynamics at high speed in mouse and zebrafish brain with confocal light field microscopy. *Nat Biotechnol* 39(1): 74–83
- Zhao Z, Zhou Y, Liu B, He J, Zhao J, Cai Y, Fan J, Li X, Wang Z, Lu Z, Wu J, Qi H, Dai Q (2023) Two-photon synthetic aperture microscopy for minimally invasive fast 3D imaging of native subcellular behaviors in deep tissue. *Cell* 186(11): 2475–2491. e22
- Zheng G, Horstmeyer R, Yang C (2013) Wide-field, high-resolution Fourier ptychographic microscopy. *Nat Photonics* 7(9): 739–745
- Zheng Y, Wang X, Jiang Z, Xu J, Yuan R, Zhao Y, Zhang H, Liu C, Wang Q (2024) Adaptive multiscale microscope with fast zooming, extended working distance, and large field of view. *Light: Adv Manuf* 5(1): 62–74
- Zhou KC, Harfouche M, Cooke CL, Park J, Konda PC, Kreiss L, Kim K, Jönsson J, Doman T, Reamey P, Saliu V, Cook CB, Zheng M, Bechtel JP, Bègue A, McCarroll M, Bagwell J, Horstmeyer G, Bagnat M, Horstmeyer R (2023) Parallelized computational 3D video microscopy of freely moving organisms at multiple gigapixels per second. *Nat Photonics* 17(5): 442–450
- Zhu L, Sun J, Yi C, Zhang M, Huang Y, Wu S, He M, Chen L, Zhang Y, Zheng C, Chen H, Zhang Y, Li D, Fei P (2023) Adaptive-learning physics-aware light-field microscopy enables day-long and millisecond-scale super-resolution imaging of 3D subcellular dynamics. *bioRxiv*. <https://doi.org/10.1101/2023.03.15.532876>
- Zhu T, Guo Y, Zhang Y, Lu Z, Lin X, Fang L, Wu J, Dai Q (2022) Noise-robust phase-space deconvolution for light-field microscopy. *J Biomed Opt* 27(7): 076501. <https://doi.org/10.1117/1.JBO.27.7.076501>
- Zhuang P, Li C, Wu J (2021) Bayesian retinex underwater image enhancement. *Eng Appl Artif Intell* 101: 104171. <https://doi.org/10.1016/j.engappai.2021.104171>
- Ziv Y, Ghosh KK (2015) Miniature microscopes for large-scale imaging of neuronal activity in freely behaving rodents. *Curr Opin Neurobiol* 32: 141–147
- Zong W, Obenhaus HA, Skytøen ER, Eneqvist H, de Jong NL, Vale R, Jorge MR, Moser MB, Moser EI (2022) Large-scale two-photon calcium imaging in freely moving mice. *Cell* 185(7): 1240–1256. e30